

# PHASE TRANSITION OF GRAPH LAPLACIAN OF HIGH DIMENSIONAL NOISY RANDOM POINT CLOUD

XIUCAI DING AND HAU-TIENG WU

**ABSTRACT.** We systematically explore the spectral distribution of kernel-based graph Laplacian constructed from high dimensional and noisy random point cloud in the non-null setup. An interesting phase transition phenomenon is reported, which is characterized by the signal-to-noise ratio (SNR). We quantify how the signal and noise interact over different SNR regimes; for example, how signal information pops out the Marchenko-Pastur bulk. Motivated by the analysis, an adaptive bandwidth selection algorithm is provided and proved, which coincides with the common practice in real data. Simulated data is provided to support the theoretical findings. Our results paves the way towards a foundation for statistical inference of various kernel-based unsupervised learning algorithms, like eigenmap, diffusion map and their variations, for real data analysis.

## 1. INTRODUCTION

Unsupervised learning is arguably a central component, if not the holy grail, in machine learning. Among many approaches, spectral algorithms are popular and have been widely applied. Common ground of these algorithms is graph Laplacian (GL) and its eigendecomposition. However, to our knowledge, when GL is constructed from a point cloud corrupted by noise, particularly in the nonnull case, our knowledge about its full spectrum is limited. While there are various setups for GL, below, we focus ourselves on a specific setup: (1) GL is constructed from a random point cloud via a kernel; (2) the kernel used to construct GL is symmetric; (3) the random point cloud is high dimensional and noisy. By *high dimensional*, we meant the large  $p$  and large  $n$  setup, where  $p$  and  $n$  stand for the dimension and size of the point cloud respectively, and  $p = p(n)$  so that  $p/n$  is always bounded from below and above for all  $n$ . Note that (1) and (2) are common in several unsupervised learning algorithms, like eigenmap (Belkin and Niyogi, 2003), diffusion map (DM) (Coifman and Lafon, 2006) and Robust and Scalable Embedding via Landmark Diffusion (Roseland) (Shen and Wu, 2020), among many others, and (3) is often encountered in modern datasets.

We first mention that under the null case; that is, the high dimensional point cloud is purely noise, there have been several studies, like El Karoui (2010b); Cheng and Singer (2013); Do and Vu (2013); El Karoui and Wu (2015); Fan and Montanari (2019); Ding and Wu (2020), among others. In this case, the spectral distribution of GL has been relatively well known. However, under the nonnull case, there are much fewer results (El Karoui, 2010a; El Karoui and Wu, 2016; Shen and Wu, 2020), where the results are mainly quantifying the impact of high dimensional noise on GL by the operator norm. As a result, the first finite eigenvalues can be estimated, and the first finite eigenvectors of GL can be controlled by the Davis-Kahan sine theorem. However, it is not clear how the whole spectral distribution looks like. Filling this gap is critical toward establishing the statistical inference framework for unsupervised learning, at least for those spectral methods.

**1.1. Setup.** Consider i.i.d. sequences of  $\mathcal{Y} := \{\mathbf{y}_i\}_{i=1}^n \in \mathbb{R}^p$  satisfies

$$(1.1) \quad \mathbb{E}(\mathbf{y}_i) = \mathbf{0}, \quad \text{cov}(\mathbf{y}_i) = \mathbf{I}_p.$$

We assume that  $\mathcal{Y}$  consists of sub-Gaussian random vectors, i.e., for any deterministic vector  $\mathbf{a} \in \mathbb{R}^p$ , we have

$$(1.2) \quad \mathbb{E}(\exp(\mathbf{a}^\top \mathbf{y}_i)) \leq \exp(\|\mathbf{a}\|_2^2/2).$$

To simplify the discussion, we assume that  $\mathbf{y}_{i,1}$ 's are continuous random variables. In the current paper, we are mainly interested in the spiked covariance matrix model (Johnstone, 2001) with rank one spike. Specifically, we denote  $\Sigma$  as

$$(1.3) \quad \Sigma = \text{diag}\{\lambda + 1, 1, \dots, 1\}.$$

Here  $\lambda := \lambda(n) \geq 0$ , and when  $\lambda > 0$  we consider

$$(1.4) \quad \lambda \asymp n^\alpha, \quad 0 \leq \alpha < \infty.$$

The random point cloud is  $\mathcal{X} := \{\mathbf{x}_i\}_{i=1}^n$ , where

$$(1.5) \quad \mathbf{x}_i = \Sigma^{1/2} \mathbf{y}_i.$$

We adopt the setting of Ding and Wu (2020) and assume that for some constant  $0 < \gamma \leq 1$ , we have

$$(1.6) \quad \gamma \leq c_n := \frac{n}{p} \leq \gamma^{-1};$$

in other words, we focus on the large  $p$  and large  $n$  setup. Note that this spiked covariance model can be viewed as the most basic manifold model in the sense that the  $\mathbf{x}_i$  can be viewed as a point sampled from a linear manifold  $\mathbb{R}^1$  embedded in  $\mathbb{R}^p$ , and then contaminated by a high dimensional noise. Thus,  $\lambda$  represents the *signal strength* which may diverge with  $n$ . On the other hand, the *total noise* in the dataset  $\mathcal{X}$  is  $p$ , and we call  $\lambda/p$  the *signal to noise ratio* (SNR). Note that when  $\lambda = 0$ , we are working with the null case; otherwise the nonnull case. This seemingly simple linear manifold model turns out to be complicated and extremely informative toward understanding the spectral structure of GL contaminated by high dimensional noise, particularly in the nonnull case. A full exploration of the manifold model is out of the scope of this paper, and will be explored in our future work.

For the point cloud  $\mathcal{X}$  defined in (1.5), we denote its *affinity matrix* (or *kernel matrix*)  $\mathbf{W}$  as a symmetric matrix whose entries follow

$$(1.7) \quad \mathbf{W}(i, j) = \exp\left(-v \frac{\|\mathbf{x}_i - \mathbf{x}_j\|^2}{h}\right), \quad 1 \leq i, j \leq n,$$

where  $v > 0$  is the chosen parameter and  $h \equiv h(n)$  is the chosen bandwidth. In this paper, we focus on the kernel of exponential type; that is,  $f(x) = \exp(-vx)$ , where  $v > 0$  is chosen by the user. In general, the kernel function  $f(x)$  can be more general with proper properties, but to simplify the discussion, we focus on the exponential kernel. Then, we define the *transition matrix*  $\mathbf{A}$

$$(1.8) \quad \mathbf{A} = \mathbf{D}^{-1} \mathbf{W},$$

where  $\mathbf{D}$  is a diagonal matrix whose entries are defined as

$$(1.9) \quad \mathbf{D}(i, i) = \sum_{j=1}^n \mathbf{W}(i, j), \quad i = 1, 2, \dots, n.$$

We call  $\mathbf{D}$  the *degree matrix*. Note that  $\mathbf{A}$  is row-stochastic. With  $\mathbf{A}$ , the (normalized) GL is defined as

$$\mathbf{L} := \frac{1}{h}(I - \mathbf{A}).$$

Since  $\mathbf{L}$  and  $\mathbf{A}$  are related by an identity shift and scaling, we focus on studying the spectral distribution of  $\mathbf{A}$ .

**1.2. The kernel effect under the null case.** The starting point is the breakthrough work reported in [El Karoui \(2010b\)](#), the spectra of  $\mathbf{W}$ , and hence  $\mathbf{A}$  and  $\mathbf{L}$ , under the assumption that  $h = p$  and the null case,  $\lambda = 0$ , are explored. The key insight from [El Karoui \(2010b\)](#) is the *kernel effect*, which we summarize here. It is shown that under the null case, the seemingly complicated kernel matrix based on a nonlinear kernel function can be well approximated by a low rank perturbed Gram matrix, with proper normalization. Precisely, for some small constants  $\zeta > 0$  and  $\xi > 0$ , with probability at least  $1 - O(n^{-1/2-\zeta})$ , when  $n$  is sufficiently large, we have

$$\|\mathbf{W} - (c_1 p^{-1} \mathbf{X}^\top \mathbf{X} + c_2 \mathbf{I}_n + R_3)\| \leq n^{-\xi},$$

where  $\mathbf{X} \in \mathbb{R}^{p \times n}$  is the data matrix with the  $i$ -th column  $\mathbf{x}_i$ ,  $c_1, c_2 \in \mathbb{R}$ , and  $R_3$  is a low rank perturbation with rank less than or equal to 3. Detailed formula and results will be given later in the proof, like (3.5). Thus, studying the affinity matrix is closely related to studying the principal component analysis (PCA) of the dataset via the Gram matrix  $\mathbf{X}^\top \mathbf{X}$  with a low rank perturbation. As an extension of [El Karoui \(2010b\)](#), the convergence rate is provided in [Ding and Wu \(2020\)](#) under some assumptions. In the null case, more relevant results under different setups can be found in [Cheng and Singer \(2013\)](#); [Do and Vu \(2013\)](#); [El Karoui and Wu \(2015\)](#); [Fan and Montanari \(2019\)](#).

**1.3. Our contribution.** The main contribution of this paper is providing a systematic treatment of the spectral distribution of GL constructed from a high dimensional random point cloud under the nonnull assumption. We extensively expand the results reported in [El Karoui \(2010a\)](#) by applying various tools from the random matrix theory to study the spectral behavior of GL constructed from high dimensional dataset with different signal-to-noise ratios (SNR). The main difference between our work and [El Karoui \(2010a\)](#) is that we do not control the operator norm. Instead, we characterize the spectral distribution of the noisy affinity matrix, and study how the signal and noise interact; that is, we allow  $\lambda$  diverge with  $n$  in order to capture the relative strength of signal and noise.

An interesting transition phenomenon of such interaction is reported and quantified. Specifically, if the signal strength  $\lambda = \lambda(n) \asymp n^\alpha$  and the total noise energy is of order  $p$ , when the kernel is fixed and the bandwidth satisfies  $h = p$ , the spectral distribution of GL behaves differently over  $\alpha = 0$ ,  $0 < \alpha < 1$ ,  $1 \leq \alpha \leq 2$  and  $\alpha > 2$ . Roughly speaking, when  $\alpha < 1$ , we essentially only see the noise, and the spectral distribution following the Marchenko-Pastur (MP) law except few outliers and those come from the kernel effect with a proper modification; when  $\alpha > 2$ , the signal dominates and we essentially see the signal part only; when  $1 \leq \alpha \leq 2$ , the signal and noise have a strong interaction and the spectral behavior is complicated. Motivated by the analysis, we propose a bandwidth selection algorithm when noise exists, and provide a theoretical proof. It turns out that the proposed bandwidth selection algorithm coincides with the commonly applied ad hoc bandwidth selection method when researchers handle real data. To our knowledge, this result provides the first theoretical justification of that common practice.

We systematically use the following notations. For a smooth function  $f(x)$ , denote  $f^{(k)}(x)$ ,  $k = 0, 1, 2, \dots$ , to be the  $k$ -th derivative of  $f(x)$ . For two sequences  $a_n$  and  $b_n$

depending on  $n$ , the notation  $a_n = O(b_n)$  means that  $|a_n| \leq C|b_n|$  for some constant  $C > 0$ , and  $a_n = o(b_n)$  means that  $|a_n| \leq c_n|b_n|$  for some positive sequence  $c_n \downarrow 0$  as  $n \rightarrow \infty$ . We also use the notation  $a_n \asymp b_n$  if  $a_n = O(b_n)$  and  $b_n = O(a_n)$ . We summarize commonly used symbols in Table 1 for the convenience of readers.

	Symbol	Meaning
Basic	$\mathbf{I}_p$	the $p \times p$ identity matrix
	$\mathbf{e}_i$	the $i$ -th standard basis in $\mathbb{R}^p$
	$\mathbf{1}$	a vector with entries all ones
	$\ \mathbf{H}\ $	the operator norm of $\mathbf{A}$
	$\circ$	Hadamard product
	$\delta_{ij}$	Kronecker delta
Setup	$\lambda$	signal strength
	$\Sigma$	population covariance matrix defined in (1.3), i.e., $\Sigma = \lambda \mathbf{e}_1 \mathbf{e}_1^\top + \mathbf{I}_p$
	$\{\mathbf{y}_i\}$	i.i.d. $p$ -dimensional white noise satisfying (1.1) and (1.2)
	$\{\mathbf{x}_i\}$	i.i.d. $p$ -dimensional noisy data points, $\mathbf{x}_i = \Sigma^{1/2} \mathbf{y}_i$
	$\{\mathbf{x}_i^{(1)}\}$	i.i.d. $p$ -dimensional clean data points, $\mathbf{x}_i^{(1)} = \sqrt{\lambda} \mathbf{y}_i \circ \mathbf{e}_1$
	$c_n$	aspect ratio, $c_n = n/p$
Algorithm	$\mathbf{X}, \mathbf{Y}$	$p \times n$ data matrices associated with $\{\mathbf{x}_i\}$ and $\{\mathbf{y}_i\}$
	$f$	kernel function, unless otherwise specified, $f(x) = \exp(-vx)$
	$h$	bandwidth
	$\mathbf{W}, \mathbf{W}_y$	affinity matrices for $\{\mathbf{x}_i\}$ and $\{\mathbf{y}_i\}$ respectively
Measures	$\mathbf{D}, \mathbf{D}_y$	degree matrices for $\{\mathbf{x}_i\}$ and $\{\mathbf{y}_i\}$ respectively
	$\mathbf{A}, \mathbf{A}_y$	normalized affinity matrices
	$\mu_{\mathbf{H}}$	ESD of the matrix $\mathbf{A}$
Measures	$\mu_{c, \sigma^2}$	MP distribution with parameters $c$ and $\sigma^2$ defined in (2.3)
	$\nu_\lambda$	scaled and shifted MP law as defined in (2.7)
	$\gamma_\mu(j)$	the $j$ -th typical location of the probability measure $\mu$ (Definition 2.2)
Constants	$\tau \equiv \tau(\lambda)$	$2(\lambda/p + 1)$
	$\varsigma \equiv \varsigma(\lambda)$	$f(0) + 2f'(\tau) - f(\tau)$
Matrices	$\mathbf{W}_1$	affinity matrix for $\{\mathbf{x}_i^{(1)}\}$
	$\mathbf{W}_{a_1}$	$f(2)\mathbf{W}_1 + (1 - f(2))\mathbf{I}_n$
	$\mathbf{P}_x$	a $n \times n$ system matrix whose entries are $\mathbf{P}_x(i, j) = \delta_{ij} \frac{\mathbf{x}_i^\top \mathbf{x}_j}{p}$
	$\mathbf{O}_x$	a $n \times n$ system matrix whose entries are $\mathbf{O}_x(i, j) = \delta_{ij} \left( \frac{\ \mathbf{x}_i\ _2^2 + \ \mathbf{x}_j\ _2^2}{p} - \tau \right)$
	$\psi$	$\psi = (\psi(1), \dots, \psi(n))^\top$ and $\psi(i) := \ \mathbf{x}_i\ _2^2 - 1$
	$\mathbf{Sh}_0$	$f(2)\mathbf{1}\mathbf{1}^\top$
	$\mathbf{Sh}_1$	$f'(2)[\mathbf{1}\psi^\top + \psi\mathbf{1}^\top]$
	$\mathbf{Sh}_2$	$\frac{f''(2)}{2} [\mathbf{1}(\psi \circ \psi)^\top + (\psi \circ \psi)\mathbf{1}^\top + 2\psi\psi^\top]$

TABLE 1. Summary of commonly used symbols

The paper is organized in the following way. The main results are described in Section 2. The preliminary results for the proof are listed in Section 3, and the proofs are given in Section 4. Some technical proofs are postponed to Appendix.

## 2. MAIN RESULTS

In this section, we state the main results of the paper.

**2.1. Some definitions.** We start with introducing the *stochastic domination* (Erdős et al., 2013). It makes precise statements of the form “ $X^{(n)}$  is bounded with high probability by  $Y^{(n)}$  up to small powers of  $n$ ”.

**Definition 2.1** (Stochastic domination). Let

$$X = \{X^{(n)}(u) : n \in \mathbb{N}, u \in U^{(n)}\}, Y = \{Y^{(n)}(u) : n \in \mathbb{N}, u \in U^{(n)}\},$$

be two families of nonnegative random variables, where  $U^{(n)}$  is a possibly  $n$ -dependent parameter set. We say that  $X$  is *stochastically dominated* by  $Y$ , uniformly in the parameter  $u$ , if for all small  $v > 0$  and large  $D > 0$ , there exists  $n_0(v, D) \in \mathbb{N}$  so that we have

$$\sup_{u \in U^{(n)}} \mathbb{P}\left(X^{(n)}(u) > n^v Y^{(n)}(u)\right) \leq n^{-D},$$

for a sufficiently large  $n \geq n_0(v, D)$ . We interchangeably use the notation  $X = O_{\prec}(Y)$  or  $X \prec Y$  if  $X$  is stochastically dominated by  $Y$ , uniformly in  $u$ , when there is no danger of confusion. In addition, we say that an  $n$ -dependent event  $\Omega \equiv \Omega(n)$  holds *with high probability* if for a  $D > 1$ , there exists  $n_0 = n_0(D) > 0$  so that

$$\mathbb{P}(\Omega) \geq 1 - n^{-D}$$

when  $n \geq n_0$ .

For any constant  $\delta \in \mathbb{R}$ , denote  $T_\delta$  to be the shifting operator that shifts a probability measure  $\mu$  defined on  $\mathbb{R}$  by  $\delta$ ; that is

$$(2.1) \quad T_\delta \mu(I) := \mu(I - \delta),$$

where  $I \subset \mathbb{R}$  is a measurable subset. Till the end of the paper, for any symmetric  $n \times n$  matrix  $\mathbf{B}$ , the eigenvalues are ordered in the decreasing fashion so that  $\lambda_1(\mathbf{B}) \geq \lambda_2(\mathbf{B}) \geq \dots \geq \lambda_n(\mathbf{B})$ .

**Definition 2.2.** For a given probability measure  $\mu$  and  $n \in \mathbb{N}$ , define the  $j$ -th *typical location* of  $\mu$  as  $\gamma_\mu(j)$ ; that is,

$$(2.2) \quad \int_{\gamma_\mu(j)}^{\infty} \mu(dx) = \frac{j}{n},$$

where  $j = 1, \dots, n$ .  $\gamma_\mu(j)$  is also called the  $j/n$ -quantile of  $\mu$ .

Let  $\mathbf{Y} \in \mathbb{R}^{p \times n}$  be the data matrix associated with the cloud points  $\mathcal{Y}$ ; that is, the  $i$ -th column  $\mathbf{Y}$  is  $\mathbf{y}_i$ . Denote the empirical spectral distribution (ESD) of  $\mathbf{Q} = \frac{\sigma^2}{p} \mathbf{Y}^\top \mathbf{Y}$  as

$$\mu_{\mathbf{Q}}(x) = \frac{1}{n} \sum_{i=1}^n \mathbf{1}_{\{\lambda_i(\mathbf{Q}) \leq x\}}, \quad x \in \mathbb{R}.$$

Here,  $\sigma > 0$  stands for the standard deviation of the scaled noise  $\sigma \mathbf{y}_i$ . It is well-known that in the high dimensional regime (1.6),  $\mu_{\mathbf{Q}}$  has the same asymptotic (Knowles and Yin, 2017) as the so-called MP law (Marchenko and Pastur, 1967), denoted as  $\mu_{c_n, \sigma^2}$ , satisfying

$$(2.3) \quad \mu_{c_n, \sigma^2}(I) = (1 - c_n)_+ \chi_I(0) + \zeta_{c_n, \sigma^2}(I),$$

where  $I \subset \mathbb{R}$  is a measurable set,  $\chi_I$  is the indicator function and  $(a)_+ := 0$  when  $a \leq 0$  and  $(a)_+ := a$  when  $a > 0$ ,

$$(2.4) \quad d\zeta_{c_n, \sigma^2}(x) = \frac{1}{2\pi\sigma^2} \frac{\sqrt{(\lambda_+ - x)(x - \lambda_-)}}{c_n x} dx,$$

$$\lambda_+ = (1 + \sigma^2 \sqrt{c_n})^2 \text{ and } \lambda_- = (1 - \sigma^2 \sqrt{c_n})^2.$$

Denote

$$(2.5) \quad \tau \equiv \tau(\lambda) := 2 \left( \frac{\lambda}{p} + 1 \right)$$

and for any kernel function  $f(x)$ , define

$$(2.6) \quad \varsigma \equiv \varsigma(\lambda) := f(0) + 2f'(\tau) - f(\tau).$$

As mentioned earlier, we focus on  $f(x) = \exp(-vx)$  throughout the paper unless otherwise specified.

Till the end of this paper, we will use  $\tau$  and  $\varsigma$  for simplicity, unless we need to specify the values of  $\tau$  and  $\varsigma$  at certain points. Recall the shift operator defined in (2.1). Denote

$$(2.7) \quad \nu_\lambda = T_{\varsigma(\lambda)} \mu_{c_n, -2f'(\tau(\lambda))/c_n},$$

where  $\mu_{c_n, -2f'(\tau(\lambda))/c_n}$  is the MP law defined in (2.3) by replacing  $\sigma^2$  with  $-2f'(\tau(\lambda))/c_n$ .

**2.2. Spectrum of kernel affinity matrices with a fixed bandwidth  $h = p$ .** In this subsection, we focus on the discussion of the spectrum of  $\mathbf{W}$  when the bandwidth is fixed as  $h = p$ . Such a choice has appeared in many works regarding the purely noisy cloud point; for instance, see El Karoui (2010b); Ding and Wu (2020), where the total noise is of order  $p$ , and El Karoui and Wu (2015), where the total noise can be larger and the “connection” may be combined with the affinity.

We start with some definitions. Let  $\mathbf{x}_i^{(1)}, i = 1, 2, \dots, n$ , be the cloud points such that  $\mathbf{x}_i^{(1)} = \sqrt{\lambda} \mathbf{y}_i \circ \mathbf{e}_1$ , which represents the signal part. Denote the matrix  $\mathbf{W}_1 \in \mathbb{R}^{n \times n}$  such that

$$(2.8) \quad \mathbf{W}_1(i, j) = \exp \left( -v \frac{\|\mathbf{x}_i^{(1)} - \mathbf{x}_j^{(1)}\|_2^2}{p} \right),$$

where  $v > 0$ . Let  $\mathbf{W}_y$  be the affinity matrix associated with the point cloud  $\mathcal{Y}$ , which represents the noise part. Note that we can separate the signal part and the noise part using the Hadamard product. Specifically, we can exactly write

$$(2.9) \quad \mathbf{W} = \mathbf{W}_1 \circ \mathbf{W}_y,$$

where  $\circ$  stands for the Hadamard product. The above representation provides a basic relation between the “signal” and “noise” parts. We comment that for a more general kernel, like a polynomial kernel, we may have a similar decomposition with some twists. See (5.3) in the Discussion section.

With the above preparation, we now state the main results regarding the spectrum of the affinity matrix  $\mathbf{W}$  under various regimes of  $\lambda$ ; that is, under different SNR’s. In the first result, we consider the case when  $\lambda$  is bounded from above; that is,  $\alpha = 0$ . This includes the *subcritical* and *supercritical* regimes.

**Theorem 2.3** (Bounded regime). Suppose (1.1)–(1.9) hold true. For some small fixed constants  $\theta > 0$  and  $\vartheta > \theta$ , when  $n$  is sufficiently large, we have that the followings hold with probability at least  $1 - O(n^{-1/2})$ :

- (1) (Subcritical regime) When  $0 < \lambda \leq \sqrt{c_n}$ , we have that for some constants  $C, C_1 > 0$ ,

$$(2.10) \quad |\lambda_{i+3}(\mathbf{W}) - \gamma_{\nu_0}(i)| \leq \begin{cases} Cn^{-1/9+2\vartheta}, & 1 \leq i \leq C_1 n^{5/6+3\vartheta/2}; \\ Cn^{1/12+\theta} i^{-1/3}, & C_1 n^{5/6+3\vartheta/2} \leq i \leq n/2. \end{cases}.$$

Here  $\nu_0$  is defined in (2.7). Similar results as (2.10) hold for  $i \geq n/2$ .

(2) (Supercritical regime) When  $\lambda$  is a fixed constant satisfying  $\lambda > \sqrt{c_n}$ , we have that for some constants  $C, C_1 > 0$ ,

$$(2.11) \quad |\lambda_{i+4}(\mathbf{W}) - \gamma_{\nu_0}(i)| \leq \begin{cases} Cn^{-1/9+2\vartheta}, & 1 \leq i \leq C_1 n^{5/6+3\vartheta/2}; \\ Cn^{1/12+\theta} i^{-1/3}, & C_1 n^{5/6+3\vartheta/2} \leq i \leq n/2. \end{cases}.$$

Similar results as (2.11) hold for  $i \geq n/2$ .

In this bounded regime, the spectral distribution is almost like the MP distribution, except few top eigenvalues. These eigenvalues either come from the *kernel effect* that will be detailed in the proof, or the signal when the signal is in the supercritical regime. This result is not surprising, since the signal is asymptotically negligible compared with the noise.

**Remark 2.4.** Theorem 2.3 holds for a more general kernel function; that is, if (1.7) is replaced by

$$(2.12) \quad \mathbf{W}(i, j) = f\left(\frac{\|\mathbf{x}_i - \mathbf{x}_j\|^2}{h}\right), \quad 1 \leq i, j \leq n,$$

where  $f \in C^3(\mathbb{R})$  is decreasing, bounded and  $f(2) > 0$ .

Next, we state the results when the signal strength  $\lambda$  diverges with  $n$ ; that is,  $\lambda = \lambda(n) \asymp n^\alpha$ , where  $\alpha > 0$ . The spectrum of  $\mathbf{W}$  will have different properties according to the values of  $\alpha$ . In our second result, we state the conclusions when  $0 < \alpha < 1$ , which is referred to as the *slowly divergent regime*.

**Theorem 2.5** (Slowly divergent regime). Suppose (1.1)–(1.9) hold true. For some small fixed constants  $0 < \theta < 1/2 - \alpha$  and  $\theta < \vartheta < \alpha$ , when  $n$  is sufficiently large, we have that the followings hold with probability at least  $1 - O(n^{-1/2})$ :

(1) When  $0 < \alpha < 0.5$ , for some constants  $C, C_1 > 0$ , we have that:

$$(2.13) \quad |\lambda_{i+4}(\mathbf{W}) - \gamma_{\nu_0}(i)| \leq \begin{cases} C \max\{n^{-1/9+2\vartheta}, n^\theta \frac{\lambda}{\sqrt{n}}\}, & 1 \leq i \leq C_1 n^{5/6+3\vartheta/2}; \\ C \max\{n^{1/12+\theta} i^{-1/3}, n^\theta \frac{\lambda}{\sqrt{n}}\}, & C_1 n^{5/6+3\vartheta/2} \leq i \leq n/2. \end{cases}.$$

Similar results as (2.13) hold for  $i \geq n/2$ .

(2) When  $0.5 \leq \alpha < 1$ , denote

$$(2.14) \quad d \equiv d(\alpha) := \left\lceil \frac{1}{1 - \alpha} \right\rceil + 1.$$

For some constant  $C > 0$ , there exists some integer  $K$  satisfying

$$5 \leq K \leq C2^d$$

so that with high probability, for all  $1 \leq i \leq n - K$ , we have that

$$(2.15) \quad |\lambda_{i+K}(\mathbf{W}) - \gamma_{\nu_0}(i)| \leq C \max \left\{ i^{-1/3} n^{-2/3}, p^{\mathcal{B}(\alpha)}, \frac{\lambda}{p} \right\},$$

where  $\mathcal{B}(\alpha) < 0$  is defined as

$$(2.16) \quad \mathcal{B}(\alpha) = (\alpha - 1) \left( \left\lceil \frac{1}{1 - \alpha} \right\rceil + 1 \right).$$

In this slowly divergent regime, since  $\alpha < 1$ , the signal is weaker than the noise, and again it is asymptotically negligible. Thus, it is not surprising to see that the noise information dominates and the spectral distribution is almost like the MP distribution, except the first few eigenvalues. Again, like in the bounded regime, these first few eigenvalues come from the kernel effect and the signal.

**Remark 2.6.** We mention that Theorem 2.5 holds for a more general kernel function like that in (2.12).

In the previous results when  $\alpha < 1$ , the kernel function  $f$  only contribute to the measure  $\nu_0$  via (2.7) and its decay rate does not play a role in the conclusions. However, once the signal becomes stronger so that  $\alpha \geq 1$ , the kernel decay rate plays an essential role. In our third result, we consider the case when  $\alpha > 2$ . In this regime, the signal is “strong”, and we call this regime the *fast divergent regime*. Recall  $\mathbf{W}_1$  defined in (2.8). Define

$$(2.17) \quad \begin{aligned} \mathbf{W}_{a_1} &= [\exp(-2v)\mathbf{1}\mathbf{1}^\top + (1 - \exp(-2v))\mathbf{I}_n] \circ \mathbf{W}_1 \\ &= \exp(-2v)\mathbf{W}_1 + (1 - \exp(-2v))\mathbf{I}_n. \end{aligned}$$

Note that  $\mathbf{W}_{a_1}$  is simply the Hadamard product of  $\mathbf{W}_1$  and the zeroth order Taylor expansion of  $\mathbf{W}_y$  (c.f. equation (4.30)). Clearly,  $\mathbf{W}_{a_1}$  contains only the signal information.

**Theorem 2.7** (Fast divergent regime). Suppose (1.1)–(1.9) hold true. When  $\alpha > 2$ , we have that

$$(2.18) \quad \sup_{1 \leq i \leq n} |\lambda_i(\mathbf{W}) - \lambda_i(\mathbf{W}_{a_1})| \prec n^{\frac{2-\alpha}{2}}.$$

Moreover, when  $\alpha$  is larger, we can explicitly calculate the eigenvalues of  $\mathbf{W}$ . For any given constant  $t \in (0, 1)$ , if

$$(2.19) \quad \alpha > \frac{2}{t} + 1,$$

we have that with probability  $1 - O(n^{1-t(\alpha-1)/2})$ , for some constant  $C > 0$  and all  $1 \leq i \leq n$ ,

$$(2.20) \quad |\lambda_i(\mathbf{W}) - 1| \leq n \exp(-v(\lambda/p)^{1-t}).$$

In this fast divergent regime, the signal is far stronger than the noise, so it can be understood as analyzing the spectral distribution of GL when the signal is contaminated by “small” noise, while the bandwidth is “small” compared with the signal strength. When the bandwidth is too small compared with the signal, like (2.19), the decay of the kernel forces each point to be “blind” to see other points. In this case, the affinity matrix  $\mathbf{W}$  is close to an identical matrix, which leads to (2.20) and (5.5). When the signal is not that strong, we can still see some information via  $\mathbf{W}_{a_1}$  shown in (2.18), which is an interpolation of  $\mathbf{W}_1$  associated with the “clean” dataset  $\{\mathbf{x}_i^{(1)}\}$  and  $\mathbf{I}_n$  depending on  $f(2)$ , which essentially comes from the zeroth order expansion of  $\mathbf{W}_y$ .

In our fourth result, we consider the last, and the most complicated case,  $1 \leq \alpha \leq 2$ . In this regime, the signal is “moderately strong” compared with the noise, so we call it the *moderately divergent regime*. Denote  $\mathbf{W}_{a_2}$  as

$$(2.21) \quad \mathbf{W}_{a_2} := \left( \frac{2v \exp(-2v)}{p} \mathbf{Y}^\top \mathbf{Y} + 2v \exp(-4v) \mathbf{I}_n \right) \circ \mathbf{W}_1.$$

Note that compared with  $\mathbf{W}_{a_1}$ , the matrix  $\frac{2v \exp(-2v)}{p} \mathbf{Y}^\top \mathbf{Y} + 2v \exp(-4v) \mathbf{I}_n$  in  $\mathbf{W}_{a_2}$  comes from a higher order Taylor expansion of  $\mathbf{W}_y$ .

**Theorem 2.8** (Moderately divergent regime). Suppose (1.1)–(1.9) hold true. For some constant  $C > 0$ , denote  $C_\alpha$

$$C_\alpha = \begin{cases} C \log n, & \alpha = 1; \\ \min\{Cn^{\alpha-1}, n\}, & 1 < \alpha \leq 2. \end{cases}$$

For some constant  $T \leq C_\alpha$ , we have with high probability that

$$(2.22) \quad \sup_{1 \leq i \leq T} \left| \lambda_i \left( \frac{1}{n} \mathbf{W} \right) - \lambda_i \left( \frac{1}{n} \mathbf{W}_{a_1} \right) \right| \leq n^{-\alpha/2},$$

where  $\mathbf{W}_{a_1}$  is defined in (2.17). Moreover, the ESD of  $\mathbf{W}$  coincides with that of  $\mathbf{W}_{a_2}$ . Specifically, let  $m_{\mathbf{W}}(z)$  and  $m_{\mathbf{W}_{a_2}}(z)$  be the Stieltjes's transforms of  $\mathbf{W}$  and  $\mathbf{W}_{a_2}$  respectively. We have

$$(2.23) \quad \sup_{z \in \mathcal{D}} |m_{\mathbf{W}}(z) - m_{\mathbf{W}_{a_2}}(z)| \prec \frac{1}{\sqrt{n}\eta^2},$$

where  $\mathcal{D}$  is the domain of spectral parameter defined as

$$(2.24) \quad \mathcal{D} \equiv \mathcal{D}(1/4, a) := \left\{ z = E + i\eta : a \leq E \leq \frac{1}{a}, n^{-1/4+a} \leq \eta \leq \frac{1}{a} \right\}$$

and  $0 < a < 1$  is some fixed (small) constant.

The theorem for the moderately divergent regime is more complicated than the others for an obvious reason. In this regime, the signal is strong enough to compete with the noise. However, the signal is not as strong as that in the fast divergent regime and cannot overcome the noise. Thus, the noise and signal information mixed together, which complicates the analysis and the result. From the theorem, we see that the signal is “strong” in the sense that we are able to recover the “top few” eigenvalues of the kernel matrix associated with the clean data via (2.22) after proper scaling. On the other hand, the signal is “not sufficiently strong” in the sense that the behavior of most of the eigenvalues, i.e., the bulk eigenvalues, are governed by both the signal part  $\mathbf{W}_1$  and noise part  $\mathbf{W}_y$  up to the first order Taylor expansion, i.e.,  $\mathbf{W}_{a_2}$  in (2.21). The behavior of the full spectrum is more complicated, which can be observed via the *local law* quantified by (2.23). Note that  $\mathbf{W}_{a_2}$  is the deformed  $\mathbf{W}_1$  by the high dimensional noise via the Hadamard product. To our knowledge, the spectral behavior of random matrices under the Hadamard product is less known, and it is the key toward a full understanding of this regime. Since real modern data usually lands in this regime, we will explore this critical problem in our future work.

**2.3. Phase transition.** From Theorem 2.3 to Theorem 2.8, we observe several phase transitions, which is illustrated in Figure 1. In the case when  $\lambda$  is bounded, we observe three or four outlying eigenvalues according to the magnitude of  $\lambda$ , where three of these outlying eigenvalues are from the kernel effect; see Lemma 3.3 for details. When  $\lambda$  transits from the subcritical regime to the supercritical regime, one extra outlier is generated due to the well-known *BBP transition* Baik et al. (2005) phenomenon for the spiked covariance matrix model. Moreover, the rest of the non-outlier eigenvalues still obey a shifted MP. As will be clear from the proof, in the bounded regime, studying the affinity matrix is directly related to studying PCA of the dataset via the Gram matrix; see (4.52) for details.

However, once the signal strength diverges, the spectrum of the eigenvalues of the affinity matrix behave totally differently. In PCA, under the setting of (1.3), no matter how large  $\lambda$  is, we can only observe a single outlier and its strength increases as  $\lambda$  increases. Moreover, only the first eigenvalue will be influenced by  $\lambda$  and the rest of the eigenvalues satisfy the MP law, which is independent of  $\lambda$ . Specifically, the second eigenvalue, i.e., the

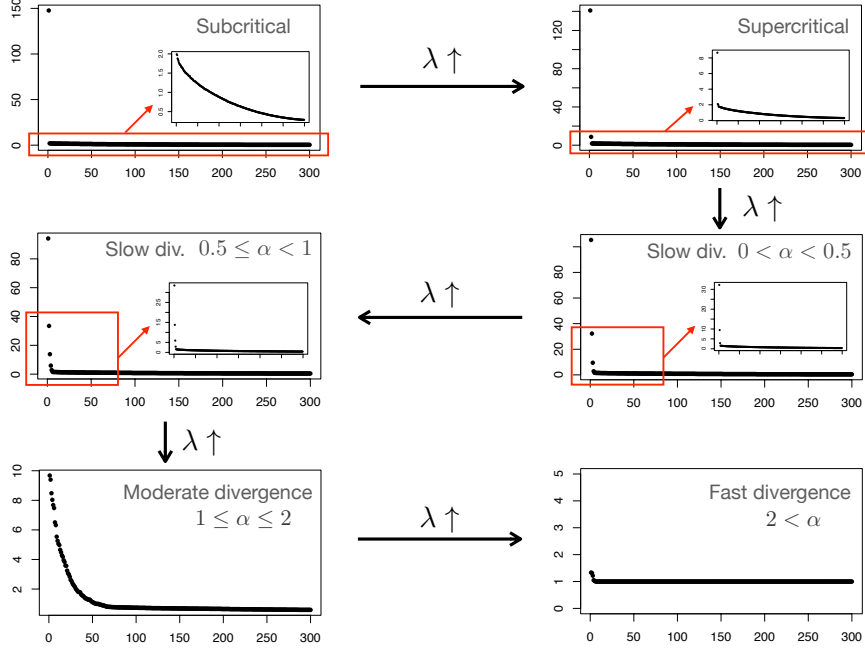


FIGURE 1. An illustration of the phase transition phenomenon of the affinity matrix spectrum. We take  $n = p = 300$ . The kernel is  $f(x) = \exp(-x/2)$  and the bandwidth is  $h = p$ . For each  $\lambda$ , the 300 eigenvalues are plotted in the descending order. In the bounded and slowly divergent regimes, the second to the 300-th eigenvalues are zoomed in for a better visualization.

first non-outlier eigenvalue will stick to the right-most edge of the MP law. We refer the readers to Lemma 3.1 for more details and Figure 2 for an illustration.

In contrast, regarding the kernel method, the values and amount of outlying eigenvalues vary according to the signal strength. That is, the magnitude of  $\lambda$  has a possible impact on *all* eigenvalues of  $\mathbf{W}$  through the kernel function. Heuristically, this is because PCA explores the point cloud in a linear fashion so that  $\lambda$  will only have an impact on the direction which explains the most variance, i.e.,  $\lambda_1(\mathbf{G})$ . However, the kernel method deals with the data in a nonlinear way such that all the eigenvalues of  $\mathbf{W}$  contain the signal information. In other words, unlike the bulk (non-outlier) eigenvalues of  $\mathbf{G}$ , all eigenvalues of  $\mathbf{W}$  change when  $\lambda$  change. Consider the following three cases. First, as we will see in the proof, the eigenvalue corresponding to the BBP transition in the supercritical regime will increase when  $\lambda$  increases, and this eigenvalue will eventually be close to one when  $\lambda$  diverges according to Theorem 2.7. Thus, when  $\alpha$  increases, we will expect the magnitude of this outlying eigenvalue to follow a bell curve. Second, the eigenvalue corresponds to the kernel effect (c.f. (3.6)) will decrease when  $\lambda$  increases since  $f$  is a decreasing function. Third, as we can see from Theorems 2.5 and 2.8, the non-outlying eigenvalues can become outlying eigenvalues when  $\lambda$  increases. In Figure 3, we illustrate the above phenomena by investigating the behavior of some eigenvalues.

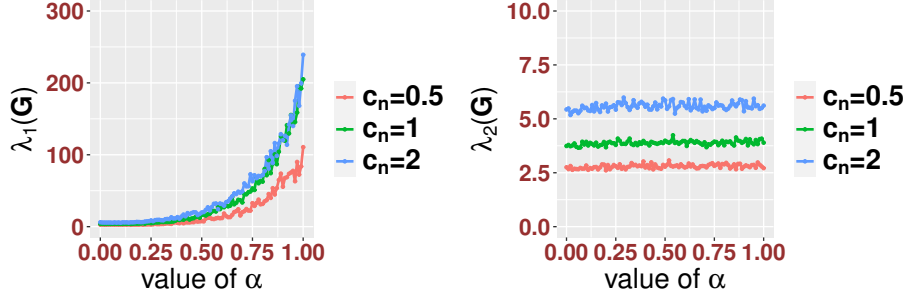


FIGURE 2. Outlier and the first non-outlier eigenvalues of  $\mathbf{G} = \frac{1}{p} \mathbf{X}^\top \mathbf{X}$ .

In this simulation, we use the Gaussian random vectors with covariance matrix (1.3) with  $\lambda = p^\alpha$  under the setting  $n = 200$  and  $c_n = n/p$ . The left panel corresponds to the first eigenvalue, i.e., the outlier eigenvalue of  $\mathbf{G}$ , and the right panel corresponds to the second eigenvalue, i.e., the first non-outlier eigenvalue, of  $\mathbf{G}$ .

**2.4. Spectrum of transition matrices with a fixed bandwidth  $h = p$ .** In what follows, we state the results for the transition matrix  $\mathbf{A}$  defined in (1.8) with a fixed bandwidth  $h = p$ . Even though there is an extra degree matrix  $\mathbf{D}$  for normalization, we claim that most of the spectrum studies of  $\mathbf{A}$  boils to those of  $\mathbf{W}$ . In fact,  $\mathbf{D}$  can be well approximated by a scalar matrix when  $\lambda$  is in the subcritical, supercritical or slowly divergent regimes. Moreover,  $\mathbf{D}$  can be well approximated by the identity matrix in the fast divergent regime when either (2.19) or (5.4) holds. In this sense, we only need to make dedicate efforts on the regime when  $\alpha$  is in the moderately divergent regime. In Figure 4, we record such a phenomenon.

We state the results in the following two corollaries. In Corollary 2.9, we present the results when  $\mathbf{D}$  can be approximated by an isotropic diagonal matrix (e.g., scalar matrix including the identity matrix).

**Corollary 2.9.** Suppose (1.1)–(1.9) hold true. Then we have the following hold:

- (1) When  $0 < \alpha < 1$ , the results of Theorems 2.3 and 2.5 can be applied to the eigenvalues of  $n\mathbf{A}$ , where  $\mathbf{W}$  is replaced by  $n\mathbf{A}$  and the measure  $\nu_0$  is replaced by

$$\check{\nu}_0 = T_{\zeta(0)} \mu_{c_n, -2f'(\tau(0))/(c_n f(\tau(\lambda)))}$$

- (2) When  $\alpha$  is sufficiently large in the sense that (2.19) holds, (2.20) can be applied directly with  $\mathbf{W}$  replaced by  $\mathbf{A}$ .

In Corollary 2.10, we state the results when  $\alpha \geq 1$  and finite. For  $\mathbf{W}_{a_1}$  defined in (2.17), denote

$$\mathbf{A}_{a_1} = \mathbf{D}_{a_1}^{-1} \mathbf{W}_{a_1},$$

where  $\mathbf{D}_{a_1}$  is the degree matrix associated with  $\mathbf{W}_{a_1}$ . Moreover, denote

$$\begin{aligned} \mathbf{W}_{a_3} &= \left( \frac{2v \exp(-2v)}{p} \mathbf{Y}^\top \mathbf{Y} + 2v \exp(-4v) \mathbf{I}_n + \exp(-2v) \mathbf{1} \mathbf{1}^\top \right) \circ \mathbf{W}_1 \\ &= \mathbf{W}_{a_2} + \exp(-2v) \mathbf{W}_1, \end{aligned}$$

and  $\mathbf{A}_{a_3} = \mathbf{D}_{a_3}^{-1} \mathbf{W}_{a_3}$ , where  $\mathbf{D}_{a_3}$  is the degree matrix associated with  $\mathbf{W}_{a_3}$ .

**Corollary 2.10.** Suppose (1.1)–(1.9) hold true. Then the following hold.

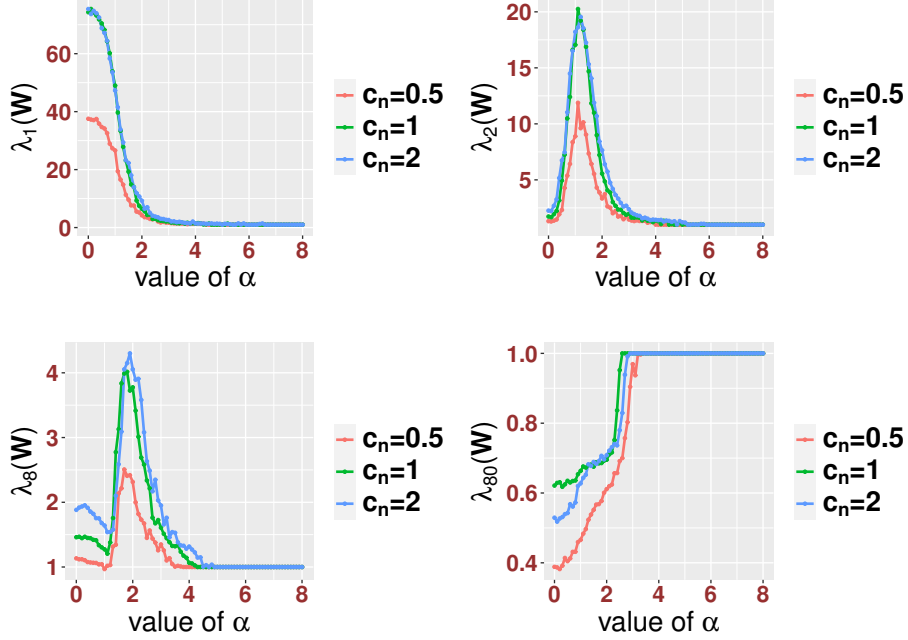


FIGURE 3. Eigenvalues of  $\mathbf{W}$  for different  $\alpha$  with the kernel  $f(x) = \exp(-x/2)$  and bandwidth  $h = p$ . In the simulation, we use the Gaussian random vectors with covariance matrix (1.3) with  $\lambda = p^\alpha$  under the setting  $n = 200$  and  $c_n = n/p$ . The top left panel corresponds to the outlying eigenvalue (i.e.  $\lambda_1(\mathbf{W})$ ) associated with  $\text{Sh}_0(\tau)$  in (3.6), the top right panel stands for the outlying eigenvalue (i.e.  $\lambda_2(\mathbf{W})$ ) from the BBP transition effect, the bottom left panel is an eigenvalue (i.e.  $\lambda_8(\mathbf{W})$ ) which gradually detaches from the bulk spectrum and becomes an outlying eigenvalue when  $\alpha$  increases. The bottom right panel is an eigenvalue sticking to the bulk spectrum (i.e.  $\lambda_{80}(\mathbf{W})$ ). In all cases, we see that the eigenvalues change when  $\alpha$  increases.

- (1) When  $\alpha > 2$  and (2.19) does not hold, (2.18) holds with  $\mathbf{W}$  and  $\mathbf{W}_{a_1}$  replaced by  $\mathbf{A}$  and  $\mathbf{A}_{a_1}$  respectively.
- (2) When  $1 \leq \alpha \leq 2$ , analogous results of Theorem 2.8 hold. Specifically, on one hand, (2.22) holds by replacing  $n^{-1}\mathbf{W}$  and  $n^{-1}\mathbf{W}_{a_1}$  with  $\mathbf{A}$  and  $\mathbf{A}_{a_1}$ , respectively; on the other hand, (2.23) holds by replacing  $\mathbf{W}$  and  $\mathbf{W}_{a_2}$  with  $\mathbf{A}$  and  $\mathbf{A}_{a_3}$ , respectively.

Note that since  $f(2) > 0$ , we can interpret that after normalization, the signal information is enhanced. However, how does this enhancement impact the spectral structure depends on the Hadamard product structure, which is out of the scope of this paper.

**2.5. Spectrum of kernel affinity matrices with adaptively chosen bandwidth.** As we have seen in Section 2.2, the spectrums of both  $\mathbf{W}$  and  $\mathbf{A}$  depend on  $\lambda$  when the bandwidth  $h$  is fixed to  $p$ . Such a simple choice of  $h$  is not sufficient for us to recover the geometric structure of the point cloud. For instance, when  $\lambda$  is in the divergent regime, this choice is

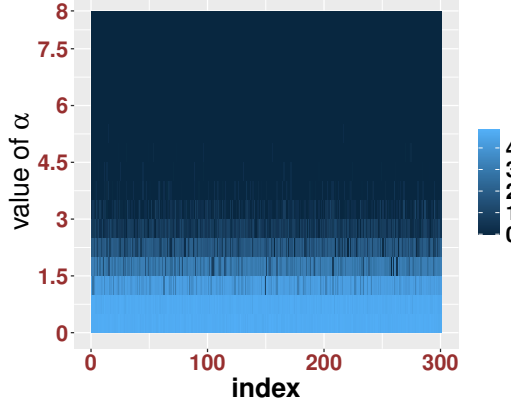


FIGURE 4. Values of the entries of  $\mathbf{D}$ . In the simulation, we use the Gaussian random vectors with  $\lambda = p^\alpha$  under the setting  $n = p = 300$ . We use a log-scale for the entries of  $\mathbf{D}$  for a better visualization. Here  $f(x) = \exp(-x/2)$  and the bandwidth is  $h = p$ . We see that when  $\alpha$  is large (e.g. empirically,  $\alpha \geq 2$ ),  $\mathbf{D}$  can be well approximated by the identity matrix. When  $\alpha$  is small (e.g. empirically,  $0 \leq \alpha < 1$ ), all the non-zero entries of  $\mathbf{D}$  seem to have the same magnitude and consequently, we can approximate  $\mathbf{D}$  using a scalar matrix. However, when  $1 \leq \alpha < 2$ , entries of  $\mathbf{D}$  seem to fluctuate.

too small and the information of the point cloud cannot be well captured. In this subsection, to address this issue, we provide an adaptive choice of  $h$  depending on the data sets. Specifically, given some constant  $\omega$ , where  $0 < \omega < 1$ , we choose  $h \equiv h(\omega)$  such that

$$(2.25) \quad \int_0^h d\mu_{\text{dist}} = \omega,$$

where  $\mu_{\text{dist}}$  is the empirical distribution of the pairwise distance  $\{\|\mathbf{x}_i - \mathbf{x}_j\|_2^2\}$ ,  $i \neq j$ . In this subsection, when there is no danger of confusion, we abuse the notation and denote the affinity and transition matrices conducted using  $h$  from (2.25) as  $\mathbf{W}$  and  $\mathbf{A}$  respectively. Moreover, denote  $\mathbf{W}_1$  according to (2.8) such that the bandwidth  $p$  is replaced by  $h$ .

**Theorem 2.11.** Suppose (1.1)–(1.9) hold true. For any  $0 < \omega < 1$ , let  $h$  be the bandwidth chosen according to (2.25). The following statements hold with probability at least  $1 - O(n^{-1/2})$ :

- (1) Assume that  $0 \leq \alpha < 1$ . Then Theorems 2.3 and 2.5 hold with  $\nu_0$  replaced by

$$\tilde{\nu}_0 = T_{\varsigma(0)} \mu_{c_n, -2pf'(\tau(\lambda))/(hc_n)}.$$

- (2) Assume that  $1 \leq \alpha \leq 2$ . Then the eigenvalues of  $\mathbf{W}$  will have analogous behavior as in the moderate regime as demonstrated in Theorem 2.8. More specifically, (2.22) holds with  $\mathbf{W}_{a_1}$  replaced by

$$(2.26) \quad \mathbf{W}_{b_1} = \left( \exp\left(-\frac{2pv}{h}\right) \mathbf{1}\mathbf{1}^\top + \left(1 - \exp\left(-\frac{2pv}{h}\right)\right) \mathbf{I} \right) \circ \mathbf{W}_1.$$

Moreover, (2.23) holds with the error bound replaced by

$$(2.27) \quad \left(\frac{p}{h}\right)^2 \frac{1}{\sqrt{n\eta^2}},$$

and  $\mathbf{W}_{a_2}$  replaced by

$$(2.28) \quad \mathbf{W}_{b_2} := \left( \frac{2pv}{h^2} \exp\left(-\frac{2pv}{h}\right) \mathbf{Y}^\top \mathbf{Y} + \frac{2pv}{h} \exp\left(-\frac{4pv}{h}\right) \mathbf{I}_n \right) \circ \mathbf{W}_1.$$

(3) When  $\alpha > 2$ , we have

$$(2.29) \quad \|\mathbf{W} - \mathbf{W}_1\| \prec \frac{p^2}{\lambda}.$$

Finally, similar results hold for the normalized affinity matrix  $\mathbf{A}$ .

According to Theorem 2.11, we find that in the bounded or slowly divergent regimes when  $\alpha < 1$ , the noise dominates and (2.25) does not play an essential role compared to the fixed bandwidth  $h = p$ . However, in the moderate or fast divergent regimes when  $\alpha \geq 1$ , the signal strength getting stronger, and the adaptive choice of bandwidth contributes significantly to the spectrum. Specifically, when  $1 \leq \alpha \leq 2$ , we can accurately estimate the outlier eigenvalues, which are contributed by the signal. However, in this case, the noise still plays a role via the Hadamard product as demonstrated in the construction of  $\mathbf{W}_{b_2}$  in (2.28). When  $\alpha > 2$ , the noise is negligible. In view of (2.18) and (2.29), different bandwidths lead to different scaling and isotropic shifts. We comment that in practice, usually researchers choose the 25% or 50% quantile of all pairwise distances, or those distances of nearest neighbor pairs, as the bandwidth. Theorem 2.11 provides a theoretical foundation for this commonly applied ad hoc bandwidth selection method.

Next, we discuss the “signal part”  $\mathbf{W}_1$  in Theorem 2.11. Note that  $\mathbf{W}_1$  is constructed with the signal  $\mathbf{x}_i^{(1)}$  but the bandwidth is determined from the noisy data. Consider  $\widetilde{\mathbf{W}}_1$ , which is modified from  $\mathbf{W}_1$  with the bandwidth  $p$  replaced by  $h_1$ , where

$$\int_0^{h_1} d\mu_{\text{dist}}^{(1)} = \omega$$

and  $\mu_{\text{dist}}^{(1)}$  is the distribution of the pairwise distance  $\{\|\mathbf{x}_i^{(1)} - \mathbf{x}_j^{(1)}\|_2^2\}$ ,  $i \neq j$ . Clearly,  $\widetilde{\mathbf{W}}_1$  is the affinity matrix constructed purely from the signal without noise contamination. If our interest is estimating the geometric structure of the signal via  $\mathbf{W}$ , it is natural to ask if we can connect  $\mathbf{W}_1$  back to  $\widetilde{\mathbf{W}}_1$ . To establish this connection, we need to study the limiting distribution of the pairwise distance instead of the empirical version and show that  $h/h_1 = 1 + o(1)$ . To our best knowledge, the limiting distribution of pairwise distance under our non-null sub-Gaussian distribution is still an open problem. The calculation needs more dedicate efforts to handle the complicated correlation and is beyond the scope of current paper. Nevertheless, we hypothesize that all the results hold if we replace  $\mathbf{W}_1$  with  $\widetilde{\mathbf{W}}_1$ , at least when the signal is sufficiently strong. We will pursue this direction in future works.

**Remark 2.12.** The simple spiked covariance model considered in this work is actually the simplest but far from trivial 1-dim manifold model. The spectral property of  $\widetilde{\mathbf{W}}_1$  constructed from clean data  $\mathbf{x}_i^{(1)}$  and a properly chosen bandwidth has been widely considered in the literature. By and large, if  $\mathbf{x}_i^{(1)}$  is “properly” sampled from  $\mathbb{R}$  embedded in  $\mathbb{R}^p$ , under some conditions on  $h_1$ , the spectral structure of the transition matrix associated with  $\widetilde{\mathbf{W}}_1$ , after a proper normalization, can well approximate the spectral structure of the heat kernel of the associated 1-dim linear manifold (Dunson et al., 2019). Via the spectral geometry theory (Bérard et al., 1994), we can recover the 1-dim manifold via the eigen-structure of  $\widetilde{\mathbf{W}}_1$ . As a result, if we can quantify the relationship between  $\widetilde{\mathbf{W}}_1$  and  $\mathbf{W}$ , we can infer how much geometric information of the 1-dim manifold we can recover. While it might

look strange to consider such a big spectral geometry machinery to analyze a 1-dim linear manifold instead of considering PCA, we mention that the whole analysis framework can be generalized to the high dimensional nonlinear structure, like nonlinear manifolds with nontrivial topologies. This idea is the essence of the manifold learning problem. A full manifold learning story will be explored in our future work.

**2.6. A new adaptive bandwidth selection algorithm.** As we can see from Theorem 2.11 and those theorems in Section 2.2, the spectrum of  $\mathbf{W}$  depends on two crucial parameters, the value of  $\lambda$  and the bandwidth  $h$ . When  $\lambda$  is much smaller than  $p$  (e.g., in the subcritical, supercritical and slowly divergent regimes), with  $h$  generated according to (2.25),  $\mathbf{W}$  will have similar spectral behavior as that demonstrated in Theorem 2.3 since  $h \asymp p$  (c.f. (4.73) in the proof) for all  $0 < \omega < 1$ . In these regimes, as we will discuss in Section 2.7, the choice of bandwidth will not influence our conclusion and we will not be able to accurately recover the geometric structure of the point cloud in this regime. When  $\lambda$  diverges, since  $h \asymp \lambda$  (c.f. (4.74) in the proof), the eigenvalues will have a moderate-type behavior demonstrated in Theorem 2.8. Roughly speaking, some of the eigenvalues will detach from the bulk and become outliers whereas the rest will be stick to the MP law with a proper scaling. Finally, since the choice of  $\omega$  will potentially have an impact on the constant  $C_1$  in (2.22), we need to properly choose an  $\omega$  such that most of the eigenfunctions can be recovered.

By the above discussion, the choice of  $\omega$  is critical for the geometric structure recovery of the point cloud. Based on the obtained theoretical results, the outliers stand for the signal information (c.f. (2.17)), except those associated with the kernel effect. Thus, we propose an algorithm to choose  $\omega$  adaptively. The algorithm is listed in Algorithm 1, where it seeks for a bandwidth so that the affinity matrix has the most number of outliers. See the numerical results shown in Section 2.7 for an example, where we will see that with a proper chosen bandwidth, we are able to recover the first few eigenfunctions of the point cloud in this regime, even when the signal is relatively weak.

---

**Algorithm 1** Adaptive choice of  $\omega$

---

- (1) Take fixed constants  $\omega_l < \omega_u$ , where  $0 < \omega_L, \omega_U < 1$ , e.g.,  $\omega_L = 0.05$  and  $\omega_U = 0.95$ . For some large integer  $T$ , we construct a partition of the intervals  $[\omega_L, \omega_U]$ , denoted as  $\mathcal{P} = (\omega_0, \omega_1, \dots, \omega_T)$ , where  $\omega_i = \omega_L + \frac{i}{T}(\omega_U - \omega_L)$ .
- (2) For the sequence of quantiles  $\{\omega_i\}_{i=0}^T$ , calculate the associated bandwidths according to (2.25), denoted as  $\{h_i\}_{i=0}^T$ .
- (3) For each  $0 \leq i \leq T$ , calculate the eigenvalues of the affinity matrices  $\mathbf{W}_i$  which is conducted using the bandwidth  $h_i$ . Denote the eigenvalues in the decreasing order as  $\{\lambda_k^{(i)}\}$ .
- (4) For a given threshold  $s > 0$  satisfying  $s \rightarrow 0$  as  $n \rightarrow \infty$ , denote

$$q_i \equiv q(\omega_i) := \max_{1 \leq k \leq n-1} \left\{ \frac{\lambda_k^{(i)}}{\lambda_{k+1}^{(i)}} \geq 1 + s \right\}.$$

Here,  $s$  is determined by the resampling method established in Ding and Yang (2020), Section 4.1.

- (5) Choose the quantile  $\omega$  such that

$$(2.30) \quad \omega = \max_{\omega_i} \arg \max_{\omega_i} q_i.$$


---

Note that we need a threshold  $s$  in step 4 of Algorithm 1. In the current paper, we adopt the resampling method established in (Ding and Yang, 2020, Section 4.1) and (Passemier and Yao, 2014, Section 4). This method will provide a choice of  $s$  to distinguish the outlier eigenvalues and bulk eigenvalues so that we can choose more outlier eigenvalues. The main reason supporting this approach is that the bulk eigenvalues are close to each other and hence the ratios of the two consecutive eigenvalues will be close to one. Moreover, in step 5 of the algorithm, when there are more than one  $\omega_i$  achieves the argmax, we choose the largest bandwidth for the purpose of robustness. In fact, when bandwidth is too small, it will amplify the values inside the kernel function, which mimics the results in the fast divergent regime.

In Figure 5, we record the choices  $\omega$  with different values of  $\alpha$ . When  $\alpha$  is smaller (empirically,  $\alpha < 1$ ), since the choice of the bandwidth will not essentially influence the transition, the algorithm will offer a large quantile in light of (2.30). When  $\lambda$  is larger (empirically,  $\alpha > 2$ ), we get a small quantile since a smaller bandwidth will generate more outliers. This finding rings the bell of existing theoretical results in manifold learning. Since the signal dominates and the noise is negligible when  $\alpha > 2$ , the affinity matrix can be well approximated by the affinity matrix from the clean signal. It is well-known that when  $n \rightarrow \infty$ , if the bandwidth decreases to 0 at a proper rate, more top eigenvalues of the affinity matrix converges to those of the heat kernel on the manifold (Dunson et al., 2019). Due to the Weyl's law, the top eigenvalues are well separated. Another interesting finding is that the choices of  $\omega$  is irrelevant of the aspect ratio  $c_n$  in (1.6). This finding suggests that the bandwidth selection is not sensitive to the ambient space dimension. A full understanding of these two findings depends on deriving the distribution of  $\mu_{\text{dist}}$  and  $\mu_{\text{dist}}^{(1)}$ , which will be explored in our future work.

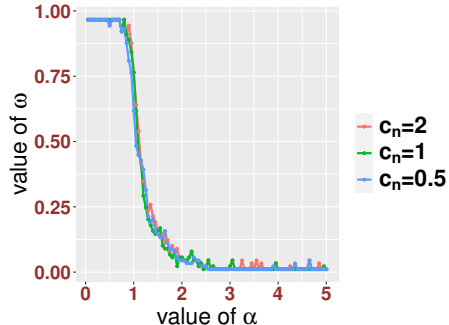


FIGURE 5. Adaptive choices of  $\omega$ . In the simulation, we use the Gaussian random vectors with  $\lambda = n^\alpha$  under the setting  $n = 200$  for different values of  $c_n$  in (1.6). The kernel function  $f(x) = \exp(-x/2)$  and the bandwidth is chosen adaptively according to (2.25), where  $\omega$  is chosen using Algorithm 1. Here, we set  $\omega_L = 0.05, \omega_U = 0.95$  and  $s = 0.12, 0.17, 0.24$  for  $c_n = 2, 1, 0.5$ , respectively.

**2.7. Application to linear manifold.** Note that the clean signal in (1.5) is sampled from the non-compact 1-dim linear manifold  $\mathbb{R}^1$  embedded in  $\mathbb{R}^p$  according to a sampling scheme following the sub-Gaussian distribution. We now consider an alternative setup, where the 1-dim linear manifold is compact. Take  $n$  independent samples  $\xi_i = (\xi_{i1}, 0, \dots, 0) \in$

$\mathbb{R}^p$ , where  $\xi_{i1} \sim \text{Uniform}(-a, a)$ . In other words, we sample uniformly from a compact manifold  $(-a, a) \subset \mathbb{R}^1$  isometrically embedded in  $\mathbb{R}^p$ . Next, we add Gaussian white noise to  $\xi_i$  via  $\mathbf{z}_i = \xi_i + \mathbf{y}_i \in \mathbb{R}^p$ , where  $\mathbf{y}_i \sim \mathcal{N}(\mathbf{0}, \mathbf{I})$ ,  $i = 1, 2, \dots, n$ , are noise independent of  $\xi_i$ . In this situation, it is easy to check that

$$\mathbb{E}(\mathbf{z}_i) = \mathbf{0}, \quad \text{Cov}(\mathbf{z}_i) = \mathbf{I} + \frac{a^2}{3}\mathbf{e}_1\mathbf{e}_1^\top.$$

With this setup, we immediately have the following corollary.

**Corollary 2.13.** Let  $\mathbf{W}$  be the affinity matrix associated with  $\{\mathbf{z}_i\}_{i=1}^n \subset \mathbb{R}^p$  conducted using (1.7). Set  $a = n^{\alpha/2}$ . When  $h = p$ , Theorems 2.3, 2.5, 2.7 and 2.8, and Corollaries 2.9 and 2.10 hold true for different  $\alpha$  with  $\lambda$  replaced by  $a^2/3$ . Analogously, when  $h$  is chosen using (2.25), Theorem 2.11 holds for different  $\alpha$  with  $\lambda$  replaced by  $a^2/3$ .

Next, we visualize the eigenvectors of  $\mathbf{W}$  with the bandwidth selection mechanism (2.25) for different values of  $\lambda$ , combined with the quantile selection method Algorithm 1. Before that, we take a closer look at the eigenstructure of  $\mathbf{W}_1$  constructed from the clean signal  $\{\xi_i\}_{i=1}^n$ . Under the current uniform sampling scheme over the linear compact manifold setup, asymptotically when  $n \rightarrow \infty$ , the top eigenvectors of  $\mathbf{W}_1$ , and hence the graph Laplacian via the degree matrix  $\mathbf{D}$ , converge to top eigenfunctions of the Laplace-Beltrami operator with the Neumann boundary condition (Coifman and Lafon, 2006). It is well known that these top eigenfunctions are sine and cosine functions with different frequencies. Thus, we would expect the top eigenvectors of  $\mathbf{W}$  to behave like sine and cosine functions. Now we come back to the illustration. According to Theorem 2.11, when  $\alpha < 1$ , most eigenvalues of  $\mathbf{W}$  or  $\mathbf{A}$  converge to the quantiles of the MP law, which only represent the information of noise. Only the first few eigenvalues may be useful for recovering the eigenfunctions of  $\mathbf{W}_1$ . Once  $\lambda \geq p$ , we see that with a proper choice of  $\omega$ , we can recover a lot of the eigenvectors of  $\mathbf{W}_1$ . In Figures 6 and 7, we record the first 9 eigenfunctions for  $\mathbf{W}$  and  $\mathbf{W}_1$  under the low SNR and large SNR settings, respectively. The bandwidths are chosen according to (2.25) together with Algorithm 1. We find that in the low SNR setting, i.e., Figure 6, only a few eigenvectors of  $\mathbf{W}_1$  can be recovered. In contrast, in the large SNR setting, i.e., Figure 7, we can accurately recover many eigenvectors of  $\mathbf{W}_1$ .

Finally, in Figure 8, we record how the choice of  $h$  influences the eigenvectors. We only consider the 7th eigenvector with various choices of  $\omega$  under the regime that  $a \geq \sqrt{3n}$ , (i.e.,  $\alpha \geq 1$  in the second statement of Theorem 2.11). We see that a smaller value of  $\omega$  will be helpful for the recovery. This supports the usefulness of Algorithm 1.

The above discussion clarify the spectral behavior of GL even under a simple and linear manifold, and we also see its non-trivial relationship with the spectral behavior of PCA. An extensive discussion of the more general manifold setup, and the eigenvector structure, is however out of the scope of this paper, and we will explore it in future work.

### 3. PRELIMINARY RESULTS

In this section, we collect some useful preliminary results, which will be used later.

**3.1. Spectral results of Gram matrices.** Denote the normalized Gram matrix of the point clouds  $\{\mathbf{x}_i\} \subset \mathbb{R}^p$  as

$$(3.1) \quad \mathbf{G} = \frac{1}{p}\mathbf{X}^\top\mathbf{X}, \quad \mathbf{X} = [\mathbf{x}_1 \cdots \mathbf{x}_n] \in \mathbb{R}^{p \times n}.$$

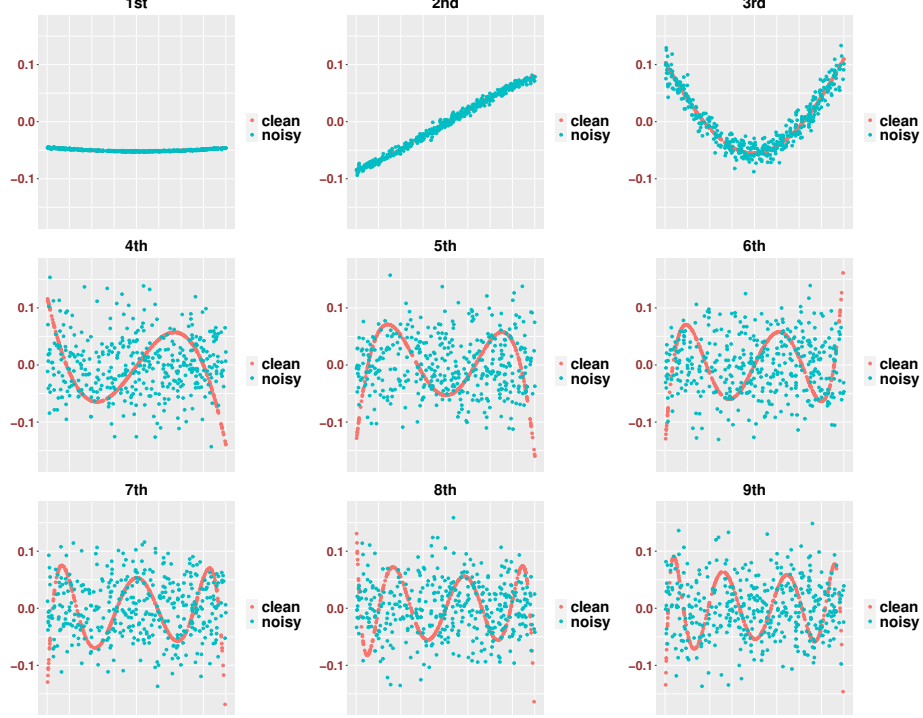


FIGURE 6. Low SNR: the first nine eigenvectors of  $\mathbf{W}_1$  from the clean data and  $\mathbf{W}$  from the noisy data. Here  $p = n = 400$ , and  $a = 20$ . The noise is Gaussian and the kernel is  $f(x) = \exp(-x/2)$ . We use Algorithm 1 to get that  $\omega = 0.84$ .

The eigenvalues of  $\mathbf{G}$  have been thoroughly studied in the literature; see [Bloemendal et al. \(2016\)](#); [Bao et al. \(2020\)](#); [Paul \(2007\)](#), among others. We summarize those relevant results in the following lemma.

**Lemma 3.1.** Suppose (1.1)–(1.6) hold true. For a fixed small  $\epsilon > 0$ , we have that for  $1 \leq i \leq (1 - \epsilon)n$ ,

$$(3.2) \quad |\lambda_{i+1}(\mathbf{G}) - \gamma_{\mu_{c_n,1}}(i)| \prec n^{-2/3}i^{-1/3}.$$

Moreover, if  $\lambda$  is in the subcritical regime, we have

$$(3.3) \quad |\lambda_1(\mathbf{G}) - \gamma_{\mu_{c_n,1}}(1)| \prec n^{-2/3},$$

and if  $\lambda$  is in the supercritical regime or larger, we have

$$(3.4) \quad \left| \lambda_1(\mathbf{G}) - (1 + \lambda) \left( 1 + \frac{c_n}{\lambda} \right) \right| \prec n^{-1/2}.$$

*Proof.* We mention that the theorems has been originally proved in [Bloemendal et al. \(2016\)](#) under a slightly different setup, and stated in current form in [Bao et al. \(2020\)](#); see Lemmas 4.6 and 4.7 therein.  $\square$

### 3.2. Some spectral bounds for affinity matrices.

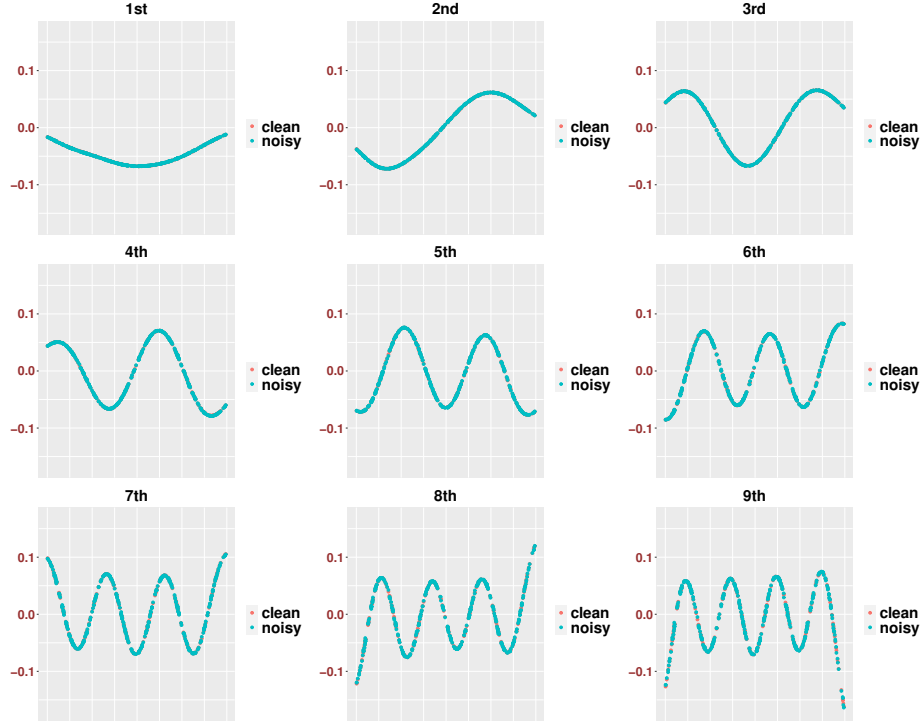


FIGURE 7. Large SNR: the first nine eigenfunctions of  $\mathbf{W}_1$  from the clean data and  $\mathbf{W}$  from the noisy data. Here  $p = n = 400$ , and  $a = 20\sqrt{p}$ . The noise is Gaussian and the kernel is  $f(x) = \exp(-x/2)$ . We use Algorithm 1 to get that  $\omega = 0.1$ . Clearly, the eigenvectors of  $\mathbf{W}$  and  $\mathbf{W}_1$  are close and it is difficult to distinguish them. We mention that since these are eigenvectors of  $\mathbf{W}$  without a normalization by  $\mathbf{D}$ , they are deviated from the sine and cosine functions near the boundary.

**Lemma 3.2.** Suppose (1.1)–(1.9) hold true,  $\alpha = 0$  in (1.4) (i.e.,  $\lambda$  is bounded) and  $h = p$  in (1.7). Let  $\Phi = (\phi_1, \dots, \phi_n)$  with  $\phi_i = \frac{1}{p} \|\mathbf{x}_i\|_2^2 - (1 + \lambda/p)$ ,  $i = 1, 2, \dots, n$ . Denote

$$(3.5) \quad \mathbf{K}_d \equiv \mathbf{K}_d(\tau) = -2f'(\tau)p^{-1}\mathbf{X}^\top\mathbf{X} + \varsigma\mathbf{I}_n + \text{Sh}_0(\tau) + \text{Sh}_1(\tau) + \text{Sh}_2(\tau),$$

where  $f(x)$  is a general kernel function satisfying the conditions in Remark 2.4,  $\varsigma$  is defined in (2.6), and

$$(3.6) \quad \begin{aligned} \text{Sh}_0(\tau) &:= f(\tau)\mathbf{1}\mathbf{1}^\top, \\ \text{Sh}_1(\tau) &:= f'(\tau)[\mathbf{1}\Phi^\top + \Phi\mathbf{1}^\top], \\ \text{Sh}_2(\tau) &:= \frac{f^{(2)}(\tau)}{2} \left[ \mathbf{1}(\Phi \circ \Phi)^\top + (\Phi \circ \Phi)\mathbf{1}^\top + 2\Phi\Phi^\top + 4\frac{(\lambda + 1)^2 + p}{p^2}\mathbf{1}\mathbf{1}^\top \right], \end{aligned}$$

and  $\circ$  is the Hadamard product. Then for some small constant  $\xi > 0$ , when  $n$  is sufficiently large, we have that with probability at least  $1 - O(n^{-1/2})$

$$(3.7) \quad \|\mathbf{W} - \mathbf{K}_d\| \leq n^{-1/4+\xi}.$$

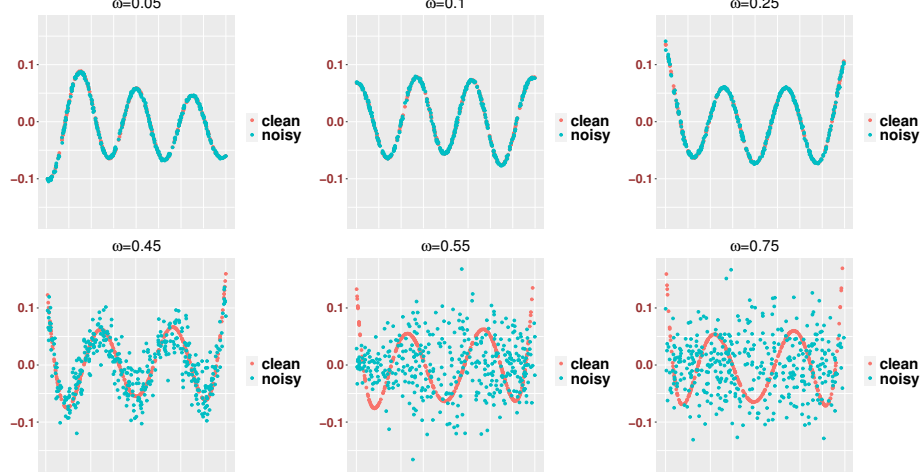


FIGURE 8. Comparison of the seventh eigenvector of  $\mathbf{W}$  with different bandwidths. Here  $p = n = 400$  and  $a = 10\sqrt{p}$ . We use the Gaussian random vector as the noise component and  $f(x) = \exp(-x/2)$  as our kernel function. If we run the proposed bandwidth selection algorithm, we get  $\omega = 0.09$ .

*Proof.* In [El Karoui \(2010b\)](#), the author stated the result without keeping track of the probability and focused on a more general setup. Our proof relies on the proof of [\(El Karoui, 2010b, Theorem 2.2\)](#) by keeping track of the detailed probability and using the concentration inequality, Lemma [A.1](#), for the Sub-Gaussian random variables.  $\square$

Moreover, when  $\lambda = 0$  in [\(1.3\)](#) such that the observations are white noise  $\{\mathbf{y}_i\}$  and  $\tau = 2$  in [\(2.5\)](#), we get the following rigidity result of eigenvalues.

**Lemma 3.3.** Suppose [\(1.1\)–\(1.9\)](#) hold true with  $\lambda = 0$  and  $h = p$  in [\(1.7\)](#). For some constants  $C, C_1 > 0$  and small fixed constants  $\theta > 0$  and  $\vartheta > \theta$ , when  $n$  is sufficiently large, with probability at least  $1 - O(n^{-1/2})$ , we have

$$\left| \lambda_i \left( \mathbf{W}_y - \sum_{k=0}^2 \text{Sh}_k(2) \right) - \gamma_{\nu_0}(i) \right| \leq \begin{cases} Cn^{-1/9+2\vartheta} & 1 \leq i \leq C_1 n^{5/6+3\vartheta/2}; \\ Cn^{1/12+\theta} i^{-1/3} & C_1 n^{5/6+3\vartheta/2} \leq i \leq n/2. \end{cases}$$

Similar results hold true for  $i \geq n/2$ .

*Proof.* See [Ding and Wu \(2020\)](#), Theorem 3.2.  $\square$

The following lemma provides a control for the Hadamard product. In [El Karoui \(2010b\)](#), the author stated the result without keeping track of the probability and focuses on a general  $\Sigma$ . In our setup with the white noise  $\mathcal{Y}$ , we can extract the probability and bounds by tracking the proof in [El Karoui \(2010b\)](#); see Step (iv) therein.

**Lemma 3.4.** Suppose [\(1.1\)–\(1.9\)](#) hold true and  $h = p$  in [\(1.7\)](#). Denote  $\mathbf{G}_x$  as the Gram matrix constructed from the point cloud  $\mathcal{X}$ . We further denote

$$(3.8) \quad \tilde{\mathbf{G}}_x = \mathbf{G}_x - \text{diag}\{\mathbf{G}_x(1, 1), \dots, \mathbf{G}_x(n, n)\}.$$

For some constant  $C > 0$ , when  $n$  is sufficiently large, with probability at least  $1 - O(n^{-1/2})$ , we have

$$\left\| \tilde{\mathbf{G}}_x \circ \tilde{\mathbf{G}}_x - \frac{(\lambda + 1)^2 + p - 1}{p^2} (\mathbf{1}\mathbf{1}^\top - \mathbf{I}_n) \right\| \leq C \max \left\{ n^{-1/4}, \frac{\lambda}{p} \right\}.$$

Finally, we record some linear algebraic results for Hadamard product from [El Karoui \(2010b\)](#), Lemma A.5.

**Lemma 3.5.** Suppose  $\mathbf{M}$  is a real symmetric matrix with nonnegative entries and  $\mathbf{E}$  is a real symmetric matrix. Then we have that

$$\sigma_1(\mathbf{M} \circ \mathbf{E}) \leq \max_{i,j} |\mathbf{E}(i,j)| \sigma_1(\mathbf{M}),$$

where  $\sigma_1(\mathbf{M})$  stands for the largest singular value of  $\mathbf{M}$ .

We also need the following lemma, which is of independent interest.

**Lemma 3.6.** Suppose (1.1)–(1.9) hold true and  $\alpha \geq 1$ . For the matrix  $\mathbf{W}_1$  associated with the clean signal defined in (2.8) and  $\delta > 0$ , with high probability, we have

$$(3.9) \quad \|\mathbf{W}_1\| \leq (n - n^\delta) \exp(-n^{\alpha-1-2(1-\delta)}) + n^\delta.$$

*Proof.* For an arbitrarily small constant  $\epsilon > 0$  and a given  $\delta > 0$ , let  $C_\delta > 0$  be some constant, and denote the event  $\mathcal{A}(\delta)$  as

$$\mathcal{A}(\delta) := \{ \text{There exists } C_\delta n^\delta \mathbf{y}'_{i1} s \text{ such that } |\mathbf{y}_{i1}| \leq n^{-\epsilon} \},$$

Denote  $\ell := \mathbb{P}(|\mathbf{y}_{i1}| \leq n^{-\epsilon})$ . Due to the independence, we find that

$$(3.10) \quad \mathbb{P}(\mathcal{A}(\delta)) = \binom{n}{C_\delta n^\delta} \ell^{C_\delta n^\delta} (1 - \ell)^{n - C_\delta n^\delta}.$$

Using Stirling's formula, when  $n$  is sufficiently large, we find that

$$\begin{aligned} \binom{n}{C_\delta n^\delta} &= \frac{n!}{(n - C_\delta n^\delta)!(C_\delta n^\delta)!} \\ &\asymp \sqrt{2\pi n}^{n+1/2} \exp(-n) (C_\delta n^\delta)^{-C_\delta n^\delta - 1/2} \exp(C_\delta n^\delta) \\ &\quad \times (n - C_\delta n^\delta)^{-n + C_\delta n^\delta - 1/2} \exp(n - C_\delta n^\delta) \\ &\asymp \sqrt{\frac{2\pi}{C_\delta}} \sqrt{\frac{n^{1-\delta}}{n - C_\delta n^\delta}} \left(1 + \frac{C_\delta n^\delta}{n - n^\delta}\right)^{n - C_\delta n^\delta} \left(\frac{n}{C_\delta n^\delta}\right)^{C_\delta n^\delta} \\ (3.11) \quad &\asymp \sqrt{\frac{2\pi}{C_\delta}} n^{(1-\delta)C_\delta n^\delta - \delta/2} \exp(C_\delta n^\delta). \end{aligned}$$

We next provide an estimate for  $\ell$ . Recall the assumption that  $\{\mathbf{y}_{i1}\}_{i=1}^n$  are continuous random variables. Denote the probability density function (PDF) of  $\mathbf{y}_{i1}^2$  as  $\varrho$  and the PDF of  $\mathbf{y}_{i1}^2$  is  $\tilde{\varrho}$ . By using the fact  $\varrho(y) = (\tilde{\varrho}(\sqrt{y}) + \tilde{\varrho}(-\sqrt{y}))/2\sqrt{y}$ , we find that

$$\varrho(y) \asymp O\left(\frac{1}{\sqrt{y}}\right).$$

Consequently, we have that for any small  $y > 0$ ,

$$(3.12) \quad \mathbb{P}(\mathbf{y}_{i1}^2 \leq y) \asymp O(\sqrt{y}).$$

By (3.12), we immediately have that

$$(3.13) \quad \ell \asymp n^{-\epsilon}.$$

Since  $\ell \rightarrow 0$  as  $n \rightarrow \infty$ , we have

$$(3.14) \quad \ell^{C_\delta n^\delta} (1 - \ell)^{n - C_\delta n^\delta} \asymp \exp(-\ell n) \ell^{C_\delta n^\delta}, \quad n \rightarrow \infty.$$

By plugging (3.11) and (3.14) into (3.10), we obtain

$$(3.15) \quad \begin{aligned} \mathbb{P}(\mathcal{A}(\delta)) &\asymp \exp(-\ell n + C_\delta(1 - \delta)n^\delta \log n + C_\delta n^\delta \log \ell) \\ &\asymp \exp(-n^{1-\epsilon} + C_\delta(1 - \delta)n^\delta \log n - C_\delta \epsilon n^\delta \log n + C_\delta n^\delta) \\ &= \exp(-n^{1-\epsilon} + C_\delta [1 - \delta - \epsilon + 1/\log(n)] n^\delta \log n) \end{aligned}$$

where the second asymptotic comes from plugging (3.13). In light of (3.15), to make  $\mathcal{A}(\delta)$  a high probability event, we may take  $\epsilon + \delta = 1$ , which leads to

$$\mathbb{P}(\mathcal{A}(\delta)) \asymp \exp((C_\delta - 1)n^\delta).$$

We can choose  $C_\delta > 1$  such that for any large constant  $D > 0$ , when  $n$  is large enough, we have that

$$(3.16) \quad \mathbb{P}(\mathcal{A}(\delta)) \geq 1 - n^{-D}.$$

Note that  $\mathbf{W}_1(i, j) = f((\mathbf{x}_i^{(1)} - \mathbf{x}_j^{(1)})^2/p) = f(\lambda(\mathbf{y}_{i1} - \mathbf{y}_{j1})^2/p)$ . On the event  $\mathcal{A}(\delta)$ , by Lemma A.3 and the definition of  $\mathbf{W}_1$ , we find that

$$\|\mathbf{W}_1\| \leq (n - n^\delta) \exp(-n^{\alpha-1-2(1-\delta)}) + n^\delta,$$

where in the first inequality we consider the worst scenario such that all the elements in  $\mathcal{A}(\delta)$  are either on the same row or column. This finishes the claim with high probability.  $\square$

**3.3. Orthogonal polynomials and kernel expansion.** We first recall the celebrated Mehler's formula (for instance, see equation (5) in [Ngo \(2002\)](#) or [Foata \(1978\)](#))

$$(3.17) \quad \frac{1}{\sqrt{1-t^2}} \exp\left(\frac{2txy - t^2(x^2 + y^2)}{2(1-t^2)}\right) = \sum_{n=0}^{\infty} \frac{t^n}{n!} \tilde{H}_n(x) \tilde{H}_n(y),$$

where  $\tilde{H}_m(x)$  is the *scaled Hermite polynomial* defined as

$$\tilde{H}_m(x) = \frac{H_m(x/\sqrt{2})}{\sqrt{2^n}}$$

and  $H_m(x)$  is the *standard Hermite polynomial* defined as

$$H_m(x) = (-1)^m \exp(x^2) \frac{d^m \exp(-x^2)}{dx^m}.$$

We mention that  $\tilde{H}_m(x)$  is referred to as the probabilistic version of the Hermite polynomial. We will see later from our proof that the above Mehler's formula provides a convenient way to handle the interaction term when we write the affinity matrix as a summation of rank one matrices.

#### 4. PROOF OF THE MAIN RESULTS

In the first part of this section, we prove the main results as stated in Section 2.2 when the bandwidth is fixed so that  $h = p$ . We first prove the results for the affinity matrix  $\mathbf{W}$  in Sections 4.1–4.4 and then prove the results for the normalized kernel affinity matrix  $\mathbf{A}$  in Section 4.5.

**4.1. Proof of Theorem 2.3, the bounded regime with  $h = p$ .** Recall the cloud point  $\mathcal{Y}$  satisfying (1.1) and denote  $\mathbf{W}_y$  to be the associated affinity matrix with  $h = p$ . Also recall  $\tau$  defined in (2.5). Since the proof holds for general kernel function described in Remark 2.4, we will carry out our analysis with such general kernel function  $f(x)$ .

*Proof.* We start from investigating the bulk eigenvalues. Denote  $\delta_{ij}$  to be the Kronecker delta. By the Taylor expansion, when  $i \neq j$ , we have that

$$(4.1) \quad \begin{aligned} \mathbf{W}(i, j) = & f(\tau) + f'(\tau) [\mathbf{O}_x(i, j) - 2\mathbf{P}_x(i, j)] + \frac{f^{(2)}(\tau)}{2} [\mathbf{O}_x(i, j) - 2\mathbf{P}_x(i, j)]^2 \\ & + \frac{f^{(3)}(\xi_x(i, j))}{6} [\mathbf{O}_x(i, j) - 2\mathbf{P}_x(i, j)]^3, \end{aligned}$$

where  $\mathbf{O}_x(i, j)$  and  $\mathbf{P}_x(i, j)$  are defined as

$$(4.2) \quad \mathbf{O}_x(i, j) = (1 - \delta_{ij}) \left( \frac{\|\mathbf{x}_i\|_2^2 + \|\mathbf{x}_j\|_2^2}{p} - \tau \right), \quad \mathbf{P}_x(i, j) = (1 - \delta_{ij}) \frac{\mathbf{x}_i^\top \mathbf{x}_j}{p}$$

and  $\xi_x(i, j)$  is some value between  $(\|\mathbf{x}_i\|_2^2 + \|\mathbf{x}_j\|_2^2)/p$  and  $\tau$ . Consequently, we find that  $\mathbf{W}$  can be rewritten as

$$(4.3) \quad \begin{aligned} \mathbf{W} = & f(\tau) \mathbf{1} \mathbf{1}^\top - \frac{2f'(\tau)}{p} \mathbf{X}^\top \mathbf{X} + \varsigma(\lambda) \mathbf{I} + \left[ f'(\tau) \mathbf{O}_x + \frac{f^{(2)}(\tau)}{2} \mathbf{H}_x \right. \\ & \left. + \frac{f^{(3)}(\xi_x(i, j))}{6} \mathbf{Q}_x \right] + 2f'(\tau) \left( \frac{1}{p} \text{diag}(\|\mathbf{x}_1\|^2, \dots, \|\mathbf{x}_n\|^2) - 1 \right), \end{aligned}$$

where we used the shorthand notations

$$\mathbf{H}_x(i, j) = [\mathbf{O}_x(i, j) - 2\mathbf{P}_x(i, j)]^2 \quad \text{and} \quad \mathbf{Q}_x(i, j) = [\mathbf{O}_x(i, j) - 2\mathbf{P}_x(i, j)]^3.$$

To ease the notation, we denote

$$(4.4) \quad \widetilde{\mathbf{W}} := -\frac{2f'(\tau)}{p} \mathbf{X}^\top \mathbf{X} + \varsigma(\lambda) \mathbf{I}_n.$$

Further, we can conduct the Taylor expansion for  $\mathbf{W}_y$  similar to (4.1) by replacing  $\mathcal{X}$  by  $\mathcal{Y}$  and  $\tau$  by 2, respectively. The other quantities  $\mathbf{O}_y$ ,  $\mathbf{P}_y$  and  $\widetilde{\mathbf{W}}_y$  can be defined analogously as in (4.2) and (4.4).

Recall (3.6) and denote

$$\mathbf{W}_{-1} = \mathbf{W} - \text{Sh}_0(\tau) \quad \text{and} \quad \mathbf{W}_{y, -1} = \mathbf{W}_y - \text{Sh}_0(2).$$

Since  $f(\tau) \mathbf{1} \mathbf{1}^\top$  is at most a rank-one matrix, by Weyl's interlacing theorem, we find that

$$(4.5) \quad \lambda_{i+1}(\mathbf{W}) \leq \lambda_i(\mathbf{W}_{-1}) \leq \lambda_i(\mathbf{W})$$

for all  $1 \leq i \leq n-1$ . Thus, it suffices to study the eigenvalues of  $\mathbf{W}_{-1}$ . Similar discussion also applies to  $\mathbf{W}_{y, -1}$ . Moreover, since  $\|\text{Sh}_1(2)\| + \|\text{Sh}_2(2)\| = O_\prec(n^{-1/2})$  (see (IV.19) in Ding and Wu (2020)), the spectrum  $\mathbf{W}_{y, -1}$  is known via Lemma 3.3. It suffices to study  $\mathbf{W}_{-1}$  based on  $\mathbf{W}_{y, -1}$ . Our discussion relies on the following lemma, whose proof can be found in Section B.

**Lemma 4.1.** Under the assumptions of Theorem 2.3, we have that

$$(4.6) \quad \|(\mathbf{W}_{-1} - \widetilde{\mathbf{W}}) - (\mathbf{W}_{y, -1} - \widetilde{\mathbf{W}}_y)\| \prec n^{-1/2}.$$

Then we prove Theorem 2.3 using Lemma 4.1. We decompose

$$(4.7) \quad \mathbf{W}_{-1} - \mathbf{W}_{y,-1} = (\mathbf{W}_{-1} - \widetilde{\mathbf{W}}) - (\mathbf{W}_{y,-1} - \widetilde{\mathbf{W}}_y) + (\widetilde{\mathbf{W}} - \widetilde{\mathbf{W}}_y).$$

By Lemma 4.1, it remains to control the last term of the right-hand side of (4.69). Note that

(4.8)

$$\widetilde{\mathbf{W}} - \widetilde{\mathbf{W}}_y = -\frac{2f'(\tau)}{p} (\mathbf{X}^\top \mathbf{X} - \mathbf{Y}^\top \mathbf{Y}) + \frac{2f'(2) - 2f'(\tau)}{p} \mathbf{Y}^\top \mathbf{Y} + (\varsigma(\lambda) - \varsigma(0)) \mathbf{I}_n.$$

First, using the facts that  $\tau - 2 = \frac{2\lambda}{p}$  and  $\lambda$  is fixed, we have that for some constant  $C > 0$ ,

$$(4.9) \quad |f^{(k)}(2) - f^{(k)}(\tau)| \leq C \frac{\lambda}{p}, \quad k = 0, 1, 2.$$

Moreover, since  $\|p^{-1} \mathbf{Y}^\top \mathbf{Y}\| \prec 1$ , using the definition of  $\varsigma(\lambda)$  in (2.6), by (4.9), we see that

$$(4.10) \quad \left\| \frac{2f'(2) - 2f'(\tau)}{p} \mathbf{Y}^\top \mathbf{Y} + (\varsigma(\lambda) - \varsigma(0)) \mathbf{I}_n \right\| \prec p^{-1},$$

where we used the assumption that  $\lambda < \infty$ . Moreover, we find that

$$\mathbf{X}^\top \mathbf{X} - \mathbf{Y}^\top \mathbf{Y} = \mathbf{Y}^\top (\Sigma - \mathbf{I}_p) \mathbf{Y} = \lambda \mathbf{Y}^\top \mathbf{e}_1 \mathbf{e}_1^\top \mathbf{Y}$$

since  $\Sigma - \mathbf{I}_p = \lambda \mathbf{e}_1 \mathbf{e}_1^\top$ . This implies that

$$\mathcal{E}_1 := -\frac{2f'(\tau)}{p} (\mathbf{X}^\top \mathbf{X} - \mathbf{Y}^\top \mathbf{Y})$$

is a rank-one positive-definite matrix. Note that by (A.6),  $\|\mathcal{E}_1\| = \lambda + O_\prec(p^{-1/2})$ . By (4.6), (4.69), (4.8) and (4.10), we conclude that

$$(4.11) \quad \|\mathbf{W}_{-1} - (\mathbf{W}_{y,-1} + \mathcal{E}_1)\| \prec n^{-1/2}.$$

Moreover, denote

$$\mathcal{E}_2 := (f(2) - f(\tau)) \mathbf{1} \mathbf{1}^\top.$$

Note that since  $f$  is monotonically decreasing, we have that  $f(2) > f(\tau)$  whenever  $\lambda > 0$ . This implies that  $\mathcal{E}_2$  is also a rank-one positive-definite matrix. We now rewrite (4.11) as

$$\|\mathbf{W} + \mathcal{E}_2 - (\mathbf{W}_y + \mathcal{E}_1)\| \prec n^{-1/2}.$$

As a result, by Weyl's inequality and  $\gamma_{\nu_0}(i) - \gamma_{\nu_0}(i+3) \asymp n^{-1}$ , we have that

$$(4.12) \quad \lambda_{i+3}(\mathbf{W}_y) + O_\prec(n^{-1/2}) \leq \lambda_{i+1}(\mathbf{W}) \leq \lambda_i(\mathbf{W}_y) + O_\prec(n^{-1/2}).$$

Here in the second step we used the following inequalities

$$\lambda_{i+1}(\mathbf{W}) \leq \lambda_{i+1}(\mathbf{W} + \mathcal{E}_2) \leq \lambda_{i+1}(\mathbf{W}_y + \mathcal{E}_1) + O_\prec(n^{-1/2}),$$

and

$$\lambda_{i+1}(\mathbf{W}_y + \mathcal{E}_1) \leq \lambda_i(\mathbf{W}_y),$$

where we used the fact that  $\mathcal{E}_1$  and  $\mathcal{E}_2$  are rank-one positive semi-definite matrices and the inequality that  $\lambda_{i+1}(A) \leq \lambda_{i+1}(A + B)$  for any two positive semidefinite matrices  $A$  and  $B$ .

To finish the proof, note that we have outlying eigenvalues. By Lemma 3.2, we find that  $\mathbf{W} - \sum_{k=0}^2 \text{Sh}_k(\tau)$  has the same amount of outlying eigenvalues as  $-2f'(\tau)p^{-1} \mathbf{X}^\top \mathbf{X} + \varsigma \mathbf{I}_n$ . For the Gram matrix  $-2f'(\tau)p^{-1} \mathbf{X}^\top \mathbf{X}$ , by Lemma 3.1, we conclude that it has an outlier in the supercritical regime. Since  $\sum_{k=0}^2 \text{Sh}_k(\tau)$  is a matrix of rank at most three, in this sense,  $\mathbf{W}$  has at most four outlying eigenvalues in the supercritical regime and three in

the subcritical regime. The proof follows from (4.12), Lemma 3.3 and  $\sum_{k=0}^2 \text{Sh}_k(2)$  is of rank at most three. For (2.11), we only need to consider  $i \geq 4$ . Finally, for  $i = 1$  in (2.10), the proof follows from Lemma 3.2.  $\square$

**4.2. Proof of Theorem 2.5, the slowly divergent regime with  $h = p$ .** Since the proof in this subsection hold for general kernel function described in Remark 2.4, we will carry out our analysis with such general kernel function  $f(x)$ . Note that in this case,  $\tau$  defined in (2.5) is still bounded from above. So for a fixed  $K \in \mathbb{N}$ , the first  $K$  coefficients in the Taylor expansion can be well controlled under the smoothness assumption, i.e.,  $f^{(k)}(\tau) \asymp 1$ , for  $k = 1, 2, \dots, K$  for  $K \in \mathbb{N}$ . However, Lemma 3.2 is invalid since  $\alpha > 0$ . On the other hand, in this regime, although the concentration inequality (c.f. Lemma A.2) still works, its rate becomes worse as  $\lambda$  becomes larger. In El Karoui (2010b), they only need to conduct the Taylor expansion till the order of three since  $\lambda$  is fixed. In our setup, to handle the divergent  $\lambda$ , we need a high order expansion adaptive to  $\lambda$ . Thus, due to the nature of convergence rate in Lemma A.2, we will employ different proof strategies for the cases  $0 < \alpha < 0.5$  and  $0.5 \leq \alpha < 1$ . When  $\alpha$  satisfies  $0 < \alpha < 0.5$ , we will compare the Taylor expansions of  $\mathbf{W}$  and  $\mathbf{W}_y$  like what we did in the proof of Theorem 2.3. When  $\alpha$  satisfies  $0.5 \leq \alpha < 1$ , we will utilize a bootstrapping strategy to interpolate  $0.5 \leq \alpha < 1$  and  $0 < \alpha < 0.5$ . This comes from the second term of (A.7), where the concentration inequalities regarding  $\mathbf{x}_i^\top \mathbf{x}_j$ , where  $i \neq j$ , have different upper bounds with different  $\alpha$ .

**Proof of case (1),  $0 < \alpha < 0.5$ .** By (4.1) and Lemma A.2, we find that when  $i \neq j$ ,

$$\mathbf{W}(i, j) = f(\tau) + f'(\tau) [\mathbf{O}_x(i, j) - 2\mathbf{P}_x(i, j)] + \frac{f^{(2)}(\tau)}{2} [\mathbf{O}_x(i, j) - 2\mathbf{P}_x(i, j)]^2 + O_\prec(n^{-3/2}),$$

where we used the fact that  $f^{(3)}(\xi_x(i, j))$  is bounded. By a discussion similar to (4.3) and Lemma A.3, we find that

(4.13)

$$\mathbf{W} = f(\tau) \mathbf{1} \mathbf{1}^\top - \frac{2f'(\tau)}{p} \mathbf{X}^\top \mathbf{X} + \varsigma(\lambda) \mathbf{I} + f'(\tau) \mathbf{O}_x + \frac{f^{(2)}(\tau)}{2} \mathbf{H}_x + O_\prec(n^{-1/2}),$$

where the error quantified by  $O_\prec$  is in the operator norm. Here we used the controls that  $\mathbf{O}_x(i, j) \prec (1 - \delta_{ij})n^{-1/2}$ ,  $\mathbf{P}_x(i, j) \prec (1 - \delta_{ij})n^{-1/2}$  and Lemma A.3. Moreover, by Lemma A.2, we can control  $\mathbf{O}_x$  by

$$(4.14) \quad \|\mathbf{1}\Phi^\top + \Phi\mathbf{1}^\top - \mathbf{O}_x\| = \|2\text{diag}\{\phi_1, \dots, \phi_n\}\| \prec n^{-1/2}.$$

For  $\mathbf{H}_x$ , we write  $[\mathbf{O}_x(i, j) - 2\mathbf{P}_x(i, j)]^2 = \mathbf{O}_x(i, j)^2 + 4\mathbf{P}_x(i, j)^2 - 4\mathbf{O}_x(i, j)\mathbf{P}_x(i, j)$  and focus on the term  $\mathbf{O}_x(i, j)\mathbf{P}_x(i, j)$ . For simplicity, we define  $\mathbf{C}_x$  so that

$$\mathbf{C}_x(i, j) = \mathbf{O}_x(i, j)\mathbf{P}_x(i, j).$$

Recall (3.1). It is easy to check that (also see the proof of (El Karoui, 2010b, Theorem 2.2))

$$(4.15) \quad \mathbf{C}_x = (\mathbf{G}_x - \text{diag}(\mathbf{G}_x))\text{diag}\{\phi_1, \dots, \phi_n\} + \text{diag}\{\phi_1, \dots, \phi_n\}(\mathbf{G}_x - \text{diag}(\mathbf{G}_x)),$$

where  $\mathbf{G}_x$  is the Gram matrix constructed using the cloud point  $\mathcal{X}$ . Moreover, let  $\mathbf{G}_y$  be the Gram matrix constructed using the cloud points  $\mathcal{Y}$  and denote

$$\mathbf{F}_g = (\mathbf{G}_x - \text{diag}(\mathbf{G}_x)) - (\mathbf{G}_y - \text{diag}(\mathbf{G}_y)).$$

For  $i \neq j$ , we have that

$$\mathbf{F}_g(i, j) = \frac{\lambda}{p} \mathbf{y}_{i1} \mathbf{y}_{j1}.$$

As a result, we can further write

$$\mathbf{F}_g = \frac{\lambda}{p} (\mathbf{y} \mathbf{y}^\top - \text{diag}\{\mathbf{y}_{11}^2, \dots, \mathbf{y}_{n1}^2\}),$$

where  $\mathbf{y} := (\mathbf{y}_{11}, \dots, \mathbf{y}_{n1})^\top$ . We find that

$$\|\mathbf{F}_g\| \leq \frac{\lambda}{p} (\mathbf{y}^\top \mathbf{y} + \|\text{diag}\{\mathbf{y}_{11}^2, \dots, \mathbf{y}_{n1}^2\}\|).$$

By (A.5) and (A.6), we find that  $\|\mathbf{F}_g\| \prec \lambda$ . By Lemma 3.1 and (A.6), we find that  $\|\mathbf{G}_y - \text{diag}\{\mathbf{G}_y\}\| \prec 1$ . Consequently, we conclude that

$$\|\mathbf{G}_x - \text{diag}\{\mathbf{G}_x\}\| \prec \lambda.$$

By (4.14), we conclude that

$$\|\mathbf{C}_x\| \prec \frac{\lambda}{\sqrt{n}}.$$

With the above preparation, by (A.7),  $\mathbf{W}$  is reduced to

$$\begin{aligned} \mathbf{W} = f(\tau) \mathbf{1} \mathbf{1}^\top - \frac{2f'(\tau)}{p} \mathbf{X}^\top \mathbf{X} + \varsigma(\lambda) \mathbf{I}_n + f'(\tau) \mathbf{O}_x + \frac{f^{(2)}(\tau)}{2} \mathbf{O}_x \circ \mathbf{O}_x \\ (4.16) \quad + 2f^{(2)}(\tau) \mathbf{P}_x \circ \mathbf{P}_x + O_\prec \left( \frac{\lambda}{\sqrt{n}} \right). \end{aligned}$$

Let  $\mathbf{P}_y$  be constructed in the same way as  $\mathbf{P}_x$  in (4.2) using the cloud points  $\mathcal{Y}$ . We notice that when  $i \neq j$ , since  $\mathbf{x}_i = \Sigma^{1/2} \mathbf{y}_i$  with  $\Sigma$  defined in (1.3),

$$(4.17) \quad \frac{1}{p^2} ((\mathbf{x}_i^\top \mathbf{x}_j)^2 - (\mathbf{y}_i^\top \mathbf{y}_j)^2) = \left( \frac{\lambda}{p} \mathbf{y}_{i1} \mathbf{y}_{j1} \right) \frac{\mathbf{x}_i^\top \mathbf{x}_j + \mathbf{y}_i^\top \mathbf{y}_j}{p},$$

where we use the elementary identity  $\mathbf{x}_i^\top \mathbf{x}_j = \mathbf{y}_i^\top (\lambda \mathbf{e}_1 \mathbf{e}_1^\top + \mathbf{I}) \mathbf{y}_j$ . By (A.7), we find that

$$\frac{1}{p^2} ((\mathbf{x}_i^\top \mathbf{x}_j)^2 - (\mathbf{y}_i^\top \mathbf{y}_j)^2) \prec \frac{\lambda}{\sqrt{n}} n^{-1}.$$

Therefore, using Lemma A.3, we conclude that

$$\|\mathbf{P}_x \circ \mathbf{P}_x - \mathbf{P}_y \circ \mathbf{P}_y\| = \|\mathbf{P}_x \circ \mathbf{P}_x - \tilde{\mathbf{G}}_y \circ \tilde{\mathbf{G}}_y\| \prec \frac{\lambda}{\sqrt{n}},$$

where we used the definition (3.8). Moreover, by a discussion similar to (4.14), we can control  $\mathbf{O}_x \circ \mathbf{O}_x$  by

$$\|(\mathbf{1} \Phi^\top + \Phi \mathbf{1}^\top) \circ (\mathbf{1} \Phi^\top + \Phi \mathbf{1}^\top) - \mathbf{O}_x \circ \mathbf{O}_x\| = \|2\text{diag}\{\phi_1^2, \dots, \phi_n^2\}\| \prec n^{-1}.$$

We also notice that by the identity  $\mathbf{a} \mathbf{b}^\top \circ \mathbf{u} \mathbf{v}^\top = (\mathbf{a} \circ \mathbf{u})(\mathbf{b} \circ \mathbf{v})^\top$ , we find that

$$(4.18) \quad (\mathbf{1} \Phi^\top + \Phi \mathbf{1}^\top) \circ (\mathbf{1} \Phi^\top + \Phi \mathbf{1}^\top) = \mathbf{1} (\Phi \circ \Phi)^\top + (\Phi \circ \Phi) \mathbf{1}^\top + 2\Phi \Phi^\top$$

Combining all the above results, and applying Lemma 3.4, we get with probability at least  $1 - O(n^{-1/2})$ ,

$$\begin{aligned} \mathbf{W} = & \left( f(\tau) - 2f^{(2)}(\tau)p^{-1} \right) \mathbf{1} \mathbf{1}^\top - \frac{2f'(\tau)}{p} \mathbf{X}^\top \mathbf{X} + f'(\tau) (\mathbf{1}^\top \Phi + \Phi \mathbf{1}^\top) \\ (4.19) \quad & + \frac{f^{(2)}(\tau)}{2} (\mathbf{1} \Phi^\top + \Phi \mathbf{1}^\top) \circ (\mathbf{1} \Phi^\top + \Phi \mathbf{1}^\top) + \varsigma(\lambda) \mathbf{I}_n + O(n^\theta \frac{\lambda}{\sqrt{n}} + n^{-1/4+\theta}), \end{aligned}$$

where we used the fact that  $f^{(2)}(\tau)$  is bounded. Recall (4.4) and  $\mathbf{W}_{y,-1} = \mathbf{W}_y - f(2)\mathbf{1}\mathbf{1}^\top$ . The following lemma is an analog of Lemma 4.1. We postpone its proof into Section B.

**Lemma 4.2.** Under the assumptions of Theorem 2.3 and  $\lambda \asymp p^\alpha, 0 < \alpha < 0.5$ , we have that

$$(4.20) \quad \|(\mathbf{W}_{-1} - \widetilde{\mathbf{W}}) - (\mathbf{W}_{y,-1} - \widetilde{\mathbf{W}}_y)\| \prec \frac{\lambda}{\sqrt{n}}.$$

Armed with Lemma 4.2, by (4.19), we follow the same argument for Theorem 2.3 to conclude the proof. First, we discuss the outlying eigenvalues. Invoking (4.19), since  $\varsigma(\lambda)\mathbf{I}_n$  is simply an isotropic shift, the outlying eigenvalues of  $\mathbf{W}$  can only come from

$$(f(\tau) + 2f^{(2)}(2)p^{-1})\mathbf{1}\mathbf{1}^\top - \frac{2f'(\tau)}{p}\mathbf{X}^\top\mathbf{X} + f'(\tau)(\mathbf{1}\Phi^\top + \Phi\mathbf{1}^\top) + \frac{f^{(2)}(\tau)}{2}(\mathbf{1}\Phi^\top + \Phi\mathbf{1}^\top)\circ(\mathbf{1}\Phi^\top + \Phi\mathbf{1}^\top).$$

Using (4.18), we can rearrange the above equation to get

$$(4.21) \quad \begin{aligned} & \mathbf{1}\left[(f(\tau) + 2f^{(2)}(2)p^{-1})\mathbf{1}^\top + f'(\tau)\Phi^\top + (\Phi\circ\Phi)^\top\right] + \left[f'(\tau)\Phi + (\Phi\circ\Phi)\right]\mathbf{1}^\top \\ & + f^{(2)}(\tau)\Phi\Phi^\top - \frac{2f'(\tau)}{p}\mathbf{X}^\top\mathbf{X}. \end{aligned}$$

Note that the first three terms of (4.21) are simply rank-one matrices. Moreover, for the fourth term, since  $\lambda \gg \sqrt{c_n}$ , we conclude from Lemma 3.1 that it will cause only one outlying eigenvalue. In summary, we will at most have four outlying eigenvalues. For the bulk eigenvalues, we can repeat the discussion as for the bulk eigenvalues in Section 4.1, specifically, the discussion starting from (4.4). The only difference is that (4.19) leads to another error of order  $\lambda/\sqrt{n}$  due to the error term in (4.19). We omit further details here.  $\square$

**Proof of Case (2),  $0.5 \leq \alpha < 1$ .** For simplicity, we denote

$$(4.22) \quad \mathbf{L}_x := \mathbf{O}_x - \mathbf{P}_x.$$

By Lemma A.2, we have

$$(4.23) \quad |\mathbf{P}_x(i, j)| = O_\prec(\lambda/n) \quad |\mathbf{O}_x(i, j)| = O_\prec(\lambda/n).$$

By the Taylor expansion, when  $i \neq j$ , we have

$$(4.24) \quad \mathbf{W}(i, j) = \sum_{k=0}^{d-1} \frac{f^{(k)}(\tau)}{k!} \mathbf{L}_x(i, j)^k + \frac{f^{(d)}(\xi_x(i, j))}{d!} \mathbf{L}_x(i, j)^d,$$

where  $d$  is defined in (2.14) and  $\xi_x(i, j)$  is some value between  $(\|\mathbf{x}_i\|_2^2 + \|\mathbf{x}_j\|_2^2)/p$  and  $\tau$ . Consider  $\widetilde{\mathbf{W}}$ ,  $\mathbf{R}_d \in \mathbb{R}^{n \times n}$  defined as

$$\widetilde{\mathbf{W}}(i, j) := \sum_{k=3}^{d-1} \frac{f^{(k)}(\tau)}{k!} \mathbf{L}_x(i, j)^k, \quad \mathbf{R}_d(i, j) = \frac{f^{(d)}(\xi_x(i, j))}{d!} \mathbf{L}_x(i, j)^d$$

so that  $\mathbf{W} = \widetilde{\mathbf{W}} + \mathbf{R}_d$ . We start from claiming that

$$(4.25) \quad |\mathbf{R}_d(i, j)| \prec p^{\mathcal{B}(\alpha)-1},$$

where  $\mathcal{B}(\alpha) = (\alpha - 1) \left( \left\lceil \frac{1}{1-\alpha} \right\rceil + 1 \right) + 1$  is defined in (2.16). To see (4.25), we used (A.7) and the fact that  $d$  is finite to get

$$\mathbf{L}_x(i, j)^d \prec n^{d(-1+\alpha)} = n^{(\alpha-1)\lceil \frac{1}{1-\alpha} \rceil + \alpha - 1} = n^{\mathcal{B}(\alpha)-1}.$$

Together with (4.24), by Lemma A.3, we have that

$$\|\mathbf{R}_d\| = \left\| \mathbf{W} - \sum_{k=0}^{d-1} \frac{f^{(k)}(\tau)}{k!} \mathbf{L}_x^{\circ k} \right\| \prec n^{\mathcal{B}(\alpha)},$$

where we set

$$\mathbf{L}_x^{\circ k} := \underbrace{\mathbf{L}_x \circ \cdots \circ \mathbf{L}_x}_{k \text{ times}}.$$

Similar definition applies to  $\mathbf{O}_x^{\circ k}$  and  $\mathbf{P}_x^{\circ k}$ .

Next, we study  $\tilde{\mathbf{W}}$ . Recall the definition of  $\Phi$  in (3.6). By denoting  $\mathbf{F}_1 := \mathbf{1}\Phi^\top + \Phi\mathbf{1}^\top$  and  $\mathbf{F}_2 := -\text{diag}\{\phi_1, \dots, \phi_n\}$ , we have

$$\mathbf{O}_x = \mathbf{F}_1 + \mathbf{F}_2.$$

Clearly,  $\text{rank}(\mathbf{F}_1) = 2$ , and by Lemma A.2, we have

$$(4.26) \quad \|\mathbf{O}_x - \mathbf{F}_1\| \prec \frac{\lambda}{p}.$$

By Lemma 3.4, we find that

$$\left\| \mathbf{P}_x \circ \mathbf{P}_x - \frac{(\lambda+1)^2 + p - 1}{p^2} \mathbf{1}\mathbf{1}^\top \right\| \prec \frac{\lambda}{p}.$$

For any  $3 \leq k \leq d-1$ , in view of the expansion  $\mathbf{L}_x^{\circ k} = \sum_{l=0}^k \binom{k}{l} \mathbf{O}_x^{\circ l} \circ (-\mathbf{P}_x)^{\circ(k-l)}$ , together with the above preparation, we have the following for the term  $\mathbf{O}_x^{\circ l} \circ (-\mathbf{P}_x)^{\circ(k-l)}$ . First, when  $l = k$ , we only have the term  $\mathbf{O}_x^{\circ k}$ . By (4.26), the fact that  $d$  is bounded, and (4.23), we can replace  $\mathbf{O}_x$  by  $\mathbf{F}_1$  in the expansion of  $\tilde{\mathbf{W}}$ .

Second, when  $l = 0$ , we only have the term  $\mathbf{P}_x^{\circ k}$ . Since  $k \geq 3$ , in the case when  $k$  is an even number, we can replace  $\mathbf{P}_x^{\circ k}$  with  $\frac{(\lambda+1)^2 + p}{p^2} \mathbf{1}\mathbf{1}^\top$  by (4.23). In the case when  $k$  is an odd number, we can replace  $\mathbf{P}_x^{\circ k}$  with  $\frac{(\lambda+1)^2 + p}{p^2} \mathbf{P}_x$ , which will be absorbed in the first order expansion which contains the term  $p^{-1} \mathbf{X}^\top \mathbf{X}$  since  $\alpha < 1$ .

Third, when  $k \neq l$  and  $l \neq 0$ , we discuss a typical case when  $k = 4$  and  $l = 2$ , i.e.,  $\mathbf{O}_x^{\circ 2} \circ \mathbf{P}_x^{\circ 2}$ . Recall that

$$\mathbf{P}_x = \frac{1}{p} \mathbf{X}^\top \mathbf{X} - \frac{1}{p} \text{diag}\{\|\mathbf{x}_1\|_2^2, \dots, \|\mathbf{x}_n\|_2^2\}.$$

Since  $\Sigma = \mathbf{I} + \lambda \mathbf{e}_1 \mathbf{e}_1^\top$ , we have

$$\frac{1}{p} \mathbf{X}^\top \mathbf{X} = \frac{1}{p} \mathbf{Y}^\top (\mathbf{I} + \lambda \mathbf{e}_1 \mathbf{e}_1^\top) \mathbf{Y} = \frac{1}{p} \mathbf{Y}^\top \mathbf{Y} + \frac{\lambda}{p} \mathbf{Y}^\top \mathbf{e}_1 \mathbf{e}_1^\top \mathbf{Y} =: \frac{1}{p} \mathbf{Y}^\top \mathbf{Y} + \mathbf{T}.$$

We immediately have

$$(4.27) \quad \text{rank}(\mathbf{T}) \leq 1 \quad \text{and} \quad \max_{i,j} |\mathbf{T}(i,j)| \prec \lambda/p$$

by Lemma A.1. Consequently, we can write that

$$\begin{aligned} \mathbf{P}_x^{\circ 2} &= \mathbf{T}^{\circ 2} + \left( \frac{1}{p} \text{diag}\{\|\mathbf{x}_1\|_2^2, \dots, \|\mathbf{x}_n\|_2^2\} \right)^2 + \left( \frac{1}{p} \mathbf{Y}^\top \mathbf{Y} \circ \frac{1}{p} \mathbf{Y}^\top \mathbf{Y} \right) \\ &\quad - \frac{2}{p^2} \mathbf{Y}^\top \mathbf{Y} \circ \text{diag}\{\|\mathbf{x}_1\|_2^2, \dots, \|\mathbf{x}_n\|_2^2\} + \frac{2}{p} \mathbf{Y}^\top \mathbf{Y} \circ \mathbf{T} \\ &\quad - \frac{2}{p} \mathbf{T} \circ \text{diag}\{\|\mathbf{x}_1\|_2^2, \dots, \|\mathbf{x}_n\|_2^2\}. \end{aligned}$$

Using Lemma 3.5, the bound of  $\max_{i,j} |\mathbf{T}(i,j)|$  by (4.27), the bound of  $\max_{i,j} |\mathbf{O}_x(i,j)|$  by (A.2), and  $\max_{i,j} |\frac{1}{p} \mathbf{Y}^\top \mathbf{Y}| \prec 1$ , we have the following norm bound:

$$\|\mathbf{O}_x^{\circ 2} \circ \mathbf{P}_x^{\circ 2} - \mathbf{O}_x^{\circ 2} \circ \mathbf{T}^{\circ 2}\| = O_{\prec}(\lambda/p).$$

Together with  $\mathbf{O}_x - \mathbf{F}_1 = \text{diag}\{\phi_1, \dots, \phi_n\}$ , we have that

$$\|\mathbf{O}_x^{\circ 2} \circ \mathbf{P}_x^{\circ 2} - \mathbf{F}_1^{\circ 2} \circ \mathbf{T}^{\circ 2}\| = O_{\prec}(\lambda/p).$$

Using the simple estimate that  $\text{rank}(A \circ B) \leq \text{rank}(A) \text{rank}(B)$ , we find that

$$\text{rank}(\mathbf{F}_1^{\circ 2} \circ \mathbf{T}^{\circ 2}) \leq 2^2.$$

The other  $k$  and  $l$  can be handled in the same way. Therefore, up to an error of  $O_{\prec}(\lambda/p)$ , all the terms in  $\mathbf{L}_x^{\circ k}$ , except  $\mathbf{P}_x^{\circ k}$  that will be absorbed into the first order expansion, can be well approximated using a matrix at most of rank  $C'2^{k+1}$ , where  $0 < C' \leq 1$ . Consequently, we can find a matrix of rank at most  $C2^d$ , where  $C > 0$  to approximate  $\widetilde{\mathbf{W}}$ , which indicates that  $\widetilde{\mathbf{W}}$  will generate at most  $C2^d$  outlier eigenvalues.

To finish the spectral analysis of  $\mathbf{W}$  in (4.24), it remains to deal with the second order Taylor approximation to control the non-outlier eigenvalues follow MP law (i.e., the first order expansion involving  $\mathbf{X}^\top \mathbf{X}$ ). First, we study the Hadamard product, which is a major part of the second order terms. We need the following identity: for any  $n \times n$  matrix  $\mathbf{E}$  and vectors  $\mathbf{u}, \mathbf{v} \in \mathbb{R}^n$ ,

$$\mathbf{E} \circ \mathbf{u}\mathbf{v}^\top = \text{diag}(\mathbf{u})\mathbf{E}\text{diag}(\mathbf{v}).$$

Using the above identity, we find that

$$\begin{aligned} \mathbf{P}_x^{(K)} \circ \mathbf{P}_x^{(K)} - \mathbf{P}_y \circ \mathbf{P}_y &= \left( \frac{1}{p} \mathbf{Y}^\top (\Sigma + \mathbf{I}) \mathbf{Y} \right) \circ \frac{\lambda}{p} \mathbf{y} \mathbf{y}^\top \\ &= \frac{\lambda}{p} \text{diag}(\mathbf{y}) \left( \frac{1}{p} \mathbf{Y}^\top (\Sigma + \mathbf{I}) \mathbf{Y} \right) \text{diag}(\mathbf{y}) \end{aligned}$$

where the first equality comes from the same argument for (4.17) and we recall that  $\mathbf{y} := (\mathbf{y}_{11}, \dots, \mathbf{y}_{n1})^\top$ . Suppose the spectral decomposition of  $\frac{1}{p} \mathbf{Y}^\top (\Sigma + \mathbf{I}) \mathbf{Y}$  is

$$(4.28) \quad \frac{1}{p} \mathbf{Y}^\top (\Sigma + \mathbf{I}) \mathbf{Y} = \sum_{k=1}^{\min\{n,p\}} \alpha_k \tilde{\mathbf{u}}_k \tilde{\mathbf{u}}_k^\top.$$

With the above notation preparation, we have that

$$\begin{aligned} (4.29) \quad & \|\mathbf{P}_x^{(K)} \circ \mathbf{P}_x^{(K)} - \mathbf{P}_y \circ \mathbf{P}_y - \frac{\alpha_1 \lambda}{p} \text{diag}(\mathbf{y}) \tilde{\mathbf{u}}_1 \tilde{\mathbf{u}}_1^\top \text{diag}(\mathbf{y})\| \\ &= \left\| \frac{\lambda}{p} \text{diag}(\mathbf{y}) \left( \sum_{k=2}^{\min\{n,p\}} \alpha_k \tilde{\mathbf{u}}_k \tilde{\mathbf{u}}_k^\top \right) \text{diag}(\mathbf{y}) \right\| \leq \alpha_2 \frac{\lambda}{p} \max_i |y_{i1}^2| \prec \frac{\lambda}{p} \end{aligned}$$

where we use the fact that  $\mathbb{P}(\max_i |y_{i1}^2| > t) \leq \sum_{i=1}^p \mathbb{P}(y_{i1} > \sqrt{t}) \leq pe^{-t/2}$ . For the control of  $\alpha_2$ , observe that (4.28) is a spiked random Gram matrix with a single spike. Thus,  $\alpha_2$  is bounded using (3.2) and the fact that  $\gamma_{c,1}(1)$  is bounded. This implies that when  $0.5 \leq \alpha < 1$ , the Hadamard product of the Gram matrices can generate an extra outlier eigenvalue compared to the case  $0 < \alpha \leq 0.5$ . The rest four outlier eigenvalues will be from the first and second order terms in the Taylor expansion as in (4.21). The discussion is similar to the case of  $0 < \alpha < 0.5$  from (4.16) to (4.21). We omit the details here. Finally, we emphasize that the discussion of (4.29) is nearly optimal in light of the obtained bound.

□

**4.3. Proof of Theorem 2.7, the fast divergent regime with  $h = p$ .** In this subsection, we provide our proof for the fast divergent regime, Theorem 2.7. While the kernel is  $f(x) = \exp(-vx)$ , for notational simplicity, we keep using the symbol  $f(x)$  as the kernel function.

**Proof of (2.18).** First of all, we work on the exponential kernel function  $f(x) = \exp(-vx)$ . We start with providing some identities regarding the separation of the noise and signals. Let

$$\mathbf{C}_0 = f(2)\mathbf{1}\mathbf{1}^\top + (1 - f(2))\mathbf{I}.$$

In light of (2.17) and  $\mathbf{W}_1(i, i) = 1$ , we have

$$\mathbf{W}_{a_1} = \mathbf{C}_0 \circ \mathbf{W}_1.$$

Together with (2.9), we have

$$(4.30) \quad \mathbf{W} - \mathbf{W}_{a_1} = \mathbf{W}_1 \circ (\mathbf{W}_y - \mathbf{C}_0).$$

By Lemma 3.5 and the first order Taylor approximation of  $\mathbf{W}_y$ , we see that

$$(4.31) \quad \|\mathbf{W} - \mathbf{W}_{a_1}\| \prec \frac{1}{\sqrt{n}}\lambda_1(\mathbf{W}_1),$$

where the  $\frac{1}{\sqrt{n}}$  comes from (A.5) and (A.6). Consequently, when  $\lambda_1(\mathbf{W}_1) = o(n^{1/2})$ , we can use the eigenvalues of  $\mathbf{W}_{a_1}$  to approximate  $\mathbf{W}$ . In this sense, the study of  $\mathbf{W}$  boils down to the analysis of the affinity matrix of a scalar random variable when the operator norm of its associated kernel affinity matrix can be bounded from above. By Lemma 3.6,  $\lambda_1(\mathbf{W}_1)$  can be controlled. In order to make the first term of the right-hand side of (3.9) negligible, we take

$$\delta > \max \left\{ 0, \frac{3-\alpha}{2} \right\},$$

and hence with high probability,

$$(4.32) \quad \|\mathbf{W}_1\| = O(n^{\max\{0, \frac{3-\alpha}{2}\}}).$$

By (4.31), since  $\alpha > 2$ , with high probability we find that

$$(4.33) \quad \|\mathbf{W} - \mathbf{W}_{a_1}\| = O(n^{\max\{\frac{2-\alpha}{2}, -1/2\}}).$$

This completes the proof. □

We next deal with the case when  $\alpha$  is larger in the sense that (2.19) holds.

**Proof of (2.20).** Note that since  $\mathbf{y}_{i,1}$  are continuous random variables, it assures that with high probability, the first entry of independent  $\mathbf{y}_i$ 's are not identical with high probability. We can thus without loss of generality write

$$\mathbf{W}(i, j) = \exp \left( -v \frac{\lambda \|\mathbf{x}_i - \mathbf{x}_j\|_2^2}{p} \right).$$

Clearly,  $\frac{\lambda}{p} \asymp n^{\alpha-1}$ . We then show that for the given constant  $t \in (0, 1)$ , with probability at least  $1 - O(n^{-\delta})$ , where  $\delta > 1$ , we have

$$\frac{\|\mathbf{x}_i - \mathbf{x}_j\|_2^2}{\lambda} \geq \left( \frac{p}{\lambda} \right)^t$$

when  $i \neq j$ . By a direct expansion,

$$(4.34) \quad \frac{\|\mathbf{x}_i - \mathbf{x}_j\|_2^2}{\lambda} = \frac{\lambda + 1}{\lambda} (\mathbf{y}_{i1} - \mathbf{y}_{j1})^2 + \frac{1}{\lambda} \sum_{k=2}^p (\mathbf{y}_{ik} - \mathbf{y}_{jk})^2.$$

For the first parentheses of (4.34), note that  $\frac{1}{\lambda} (\mathbf{y}_{i1} - \mathbf{y}_{j1})^2 \prec n^{-\alpha}$ , which is dominated by  $\frac{p}{\lambda}$ . For the second parentheses of (4.34), by Lemma A.1, we find that with high probability,

$$\frac{1}{\lambda} \sum_{k=2}^p (\mathbf{y}_{ik} - \mathbf{y}_{jk})^2 \prec \frac{p}{\lambda}.$$

Thus, for  $i \neq j$ , by defining  $h_1 = \mathbf{y}_{i1} - \mathbf{y}_{j1}$ , we find that for some constant  $C > 0$ ,

$$\mathbb{P} \left( \frac{\|\mathbf{x}_i - \mathbf{x}_j\|_2^2}{\lambda} \leq \left( \frac{p}{\lambda} \right)^t \right) \leq \mathbb{P} \left( h_1^2 \leq \left( \frac{p}{\lambda} \right)^t - C \frac{p}{\lambda} \right) \leq C \left( \frac{p}{\lambda} \right)^{t/2},$$

where the final inequality comes from a discussion similar to (3.12). This leads to

$$\mathbb{P} \left( \frac{\|\mathbf{x}_i - \mathbf{x}_j\|_2^2}{\lambda} \geq \left( \frac{p}{\lambda} \right)^t \right) \geq 1 - C \left( \frac{p}{\lambda} \right)^{t/2}.$$

Note that under the condition (2.19), we have  $t(\alpha-1)/2 > 1$ , and hence  $\left( \frac{p}{\lambda} \right)^{t/2} = o(n^{-1})$ . Therefore, by Boole–Fréchet inequality, for each fixed  $i$ , we have that

$$(4.35) \quad \max_j \mathbb{P} \left( \frac{\|\mathbf{x}_i - \mathbf{x}_j\|_2^2}{\lambda} \geq \left( \frac{p}{\lambda} \right)^t \right) \geq 1 - Cn \left( \frac{p}{\lambda} \right)^{t/2}.$$

This implies that with probability at least  $1 - O(n^{1-t(\alpha-1)/2})$ , for some constant  $C > 0$ , we have that

$$(4.36) \quad \left| \sum_{j \neq i} \mathbf{W}(i, j) \right| \leq Cn \exp \left( -v \frac{\lambda}{p} \left( \frac{p}{\lambda} \right)^t \right) = Cn \exp \left( -v \left( \frac{\lambda}{p} \right)^{1-t} \right).$$

Consequently, by Lemma A.3, we conclude that with probability  $1 - O(n^{1-t(\alpha-1)/2})$

$$(4.37) \quad \|\lambda_i(\mathbf{W}) - 1\| \leq Cn \exp \left( -v \left( \frac{\lambda}{p} \right)^{1-t} \right).$$

This completes our proof.  $\square$

**4.4. Proof of Theorem 2.8, moderately divergent regime with  $h = p$ .** In this section, we prove results over the moderately divergent regime. For notational simplicity, we still keep using the symbol  $f(x) = \exp(-vx)$  as the kernel function.

*Proof.* We first deal with (2.22). Recall that we can decompose

$$(4.38) \quad \mathbf{W} = \mathbf{W}_y \circ \mathbf{W}_1.$$

In what follows, we conduct Taylor expansion for  $\mathbf{W}_y$  and Hermite polynomial expansion for  $\mathbf{W}_1$ . The Taylor expansion for  $\mathbf{W}_y$  is similar to (4.1) and we will focus on the expansion for  $\mathbf{W}_1$ . Recall  $\mathbf{x}_i^{(1)} = \sqrt{\lambda} \mathbf{y}_i \circ \mathbf{e}_1$ . By Mehler's formula (3.17), we find that when  $i \neq j$ ,

$$(4.39) \quad \mathbf{W}_1(i, j) = \sqrt{1 - t_0^2} \exp \left( \frac{3t_0^2 - 2}{2(1 - t_0^2)} (\mathbf{y}_{i1}^2 + \mathbf{y}_{j1}^2) \right) \sum_{m=0}^{\infty} \frac{t_0^m}{m!} \tilde{H}_m(\mathbf{y}_{i1}) \tilde{H}_m(\mathbf{y}_{j1}),$$

where  $t_0$  is defined

$$0 < t_0 := \frac{-v + \sqrt{v^2 + 16\beta^2/v^2}}{4(\beta/v)} < 1 \quad \text{and} \quad \beta = \lambda/p.$$

By a direct calculation, we have

$$1 - t_0^2 = \frac{v^3 \sqrt{v^2 + 16(\beta^2/v^2)} - v^4}{8\beta^2} \quad \text{and} \quad 1 - t_0 = \frac{2v}{\sqrt{v^2 + 16\beta^2/v^2} + v + 4(\beta/v)}.$$

Note that when  $\alpha > 1$ ,  $1 - t_0^2 \asymp \frac{1}{\beta}$  as  $p \rightarrow \infty$ . Therefore, with the convenience of (4.39), we find that  $\mathbf{W}_1$  can be written as an infinite summation of rank-one matrices such that

$$(4.40) \quad \mathbf{W}_1 = \sqrt{1 - t_0^2} \sum_{m=0}^{\infty} \frac{t_0^m}{m!} \mathbf{H}_m \mathbf{H}_m^{\top},$$

where  $\mathbf{H}_m \in \mathbb{R}^n$  is defined as

$$\mathbf{H}_m = \mathbf{w} \circ \tilde{\mathbf{H}}_m, \quad \tilde{\mathbf{H}}_m(i) = \tilde{H}_m(\mathbf{y}_{i1}),$$

and  $\mathbf{w} = (\mathbf{w}_1, \dots, \mathbf{w}_n)^{\top} \in \mathbb{R}^n$  is defined as

$$\mathbf{w}_i = \exp \left( \frac{3t_0^2 - 2}{2(1 - t_0^2)} \mathbf{y}_{i1}^2 \right), \quad 1 \leq i \leq n.$$

Since both  $\mathbf{y}_{i1}$  and  $\mathbf{y}_{j1}$  are sub-Gaussian random variables, for some large constants  $C, D > 0$ ,

$$(4.41) \quad \mathbb{P}(|\mathbf{y}_{i1}|^2 \leq C \log n) \geq 1 - O(n^{-D}).$$

Therefore, we conclude that with high probability, for some constant  $C_1 > 0$ ,

$$(4.42) \quad \exp \left( \frac{3t_0^2 - 2}{2(1 - t_0^2)} (\mathbf{y}_{i1}^2 + \mathbf{y}_{j1}^2) \right) \leq (\exp(C \log n))^{\frac{3t_0^2 - 2}{2(1 - t_0^2)}} \leq n^{C_1 \beta}.$$

To finish the proof, we control  $\|\mathbf{H}_m \mathbf{H}_m^{\top}\| = \|\mathbf{H}_m\|_2^2$  case by case.

**Case I:**  $\alpha = 1$ . In this case, since  $\lambda \asymp p$ , we have  $\beta \asymp 1$  and  $t_0 \in (0, 1)$  is a constant away from 1. Since the degree of  $\tilde{H}_m(x)$  is  $m \in \mathbb{N}$ , for  $x \rightarrow \infty$ , we have  $|\tilde{H}_m(x)| \sim x^m$ . Together with (4.41), we find that with high probability, for some constant  $C > 0$

$$(4.43) \quad \|\mathbf{H}_m\|_2^2 \leq n^{C_1 \beta + 1} (C \log n)^m.$$

Consequently, we have that for some constants  $C_2, C_3 > 0$ ,

$$(4.44) \quad \frac{t_0^m}{m!} \|\mathbf{H}_m\|_2^2 \leq C_3 n^{C_2 m^{-1/2}} \left( \frac{e t_0 C \log n}{m} \right)^m,$$

where we use the Stirling's formula. For notational convenience, we set

$$(4.45) \quad \mathbf{W}_1 = \mathbf{W}_{11} + \mathbf{W}_{12},$$

where

$$(4.46) \quad \mathbf{W}_{11} = \sqrt{1 - t_0^2} \sum_{m=0}^{C_0 \log n} \frac{t_0^m}{m!} \mathbf{H}_m \mathbf{H}_m^{\top}$$

and  $C_0$  will be chosen later. Now we control  $\mathbf{W}_{11}$  and  $\mathbf{W}_{12}$ . Choose a fixed large constant  $C_0 > 0$  so that  $C_0 > et_0C$ , we set  $m_0 = C_0 \log n$ . When  $n$  is large enough, by (4.44), we have that for some constants  $C_4 > 0$  and  $0 < \alpha < 1$ ,

$$(4.47) \quad \begin{aligned} \sum_{m=C_0 \log n}^{\infty} \frac{t_0^m}{m!} \|\mathbf{H}_m\|_2^2 &\leq C_3 n^{C_2} \sum_{m=C_0 \log n}^{\infty} m^{-1/2} \left( \frac{et_0C \log n}{m} \right)^m \\ &\leq C_4 n^{C_2} \int_{C_0 \log n}^{\infty} \alpha^x dx = C_4 n^{C_2} \frac{1}{\log \alpha} \alpha^{C_0 \log n}. \end{aligned}$$

This yields that for some constants  $C_5 > 0$ , with high probability

$$(4.48) \quad \sum_{m=C_0 \log n}^{\infty} \frac{t_0^m}{m!} \|\mathbf{H}_m\|_2^2 \leq C_4 \alpha^{C_0 \log n} n^{C_2} \asymp n^{-C_5 \log n + C_2}.$$

Thus, for a big constant  $D > 2$ , when  $n$  is sufficiently large, with high probability we have

$$(4.49) \quad \|\mathbf{W}_{12}\| = \left\| \mathbf{W}_1 - \sqrt{1 - t_0^2} \sum_{m=0}^{C_0 \log n} \frac{t_0^m}{m!} \mathbf{H}_m \mathbf{H}_m^\top \right\| \leq n^{-D}.$$

By a similar argument, we can show that with high probability, for any  $i, j$ ,

$$(4.50) \quad |\mathbf{W}_{12}(i, j)| = \left| \mathbf{W}_1(i, j) - \sqrt{1 - t_0^2} \sum_{m=0}^{C_0 \log n} \frac{t_0^m}{m!} \mathbf{H}_m(i) \mathbf{H}_m(j) \right| \leq n^{-D}.$$

Hence, since  $0 < \mathbf{W}_1(i, j) \leq 1$ , with high probability we obtain

$$(4.51) \quad 1 - n^{-D} \leq |\mathbf{W}_{11}(i, j)| \leq 1.$$

Recall (3.5). We observe that

$$(4.52) \quad \mathbf{W}_y \circ \mathbf{W}_1 - \mathbf{K}_d(2) \circ \mathbf{W}_{11} = (\mathbf{W}_y - \mathbf{K}_d(2)) \circ \mathbf{W}_1 + \mathbf{K}_d(2) \circ (\mathbf{W}_1 - \mathbf{W}_{11}).$$

Here, denote  $\mathbf{Y}$  to be the data matrix associated with the pure noise  $\mathcal{Y}$ . For the first term of the right-hand side of (4.52), by Lemma 3.5, we find that

$$\|(\mathbf{W}_y - \mathbf{K}_d(2)) \circ \mathbf{W}_1\| \prec n^{-1/2},$$

where we used the fact that  $|\mathbf{W}_y(i, j) - \mathbf{K}_d(2)(i, j)| \prec n^{-3/2}$  and the trivial bound  $\|\mathbf{W}_1\| \prec n$  by Lemma 3.6. The second term can be bounded similarly using (4.49). Consequently, by (4.38) we conclude that

$$\|\mathbf{W} - \mathbf{K}_d(2) \circ \mathbf{W}_{11}\| \prec n^{-1/2}.$$

Moreover, we have that

$$\begin{aligned} \mathbf{K}_d(2) \circ \mathbf{W}_{11} &= (\text{Sh}_1(2) + \text{Sh}_2(2) - 2f'(2)p^{-1}\mathbf{Y}^\top \mathbf{Y} + \varsigma \mathbf{I}_n) \circ \mathbf{W}_{11} \\ &\quad - f(2)\mathbf{W}_{12} - (1 - f(2))\mathbf{I}_n + \mathbf{W}_{a_1}. \end{aligned}$$

where we use  $\text{Sh}_0(2) \circ \mathbf{W}_{12} = f(2)\mathbf{W}_{12}$ . Moreover, we have with high probability

$$(4.53) \quad \begin{aligned} \frac{1}{n} \|(\text{Sh}_1(2) + \text{Sh}_2(2) - 2f'(2)p^{-1}\mathbf{Y}^\top \mathbf{Y} + \varsigma \mathbf{I}_n) \circ \mathbf{W}_{11}\| \\ &\leq \frac{1}{n} \|(\text{Sh}_1(2) + \text{Sh}_2(2) - 2f'(2)p^{-1}\mathbf{Y}^\top \mathbf{Y}) \circ \mathbf{W}_{11}\| + \frac{\varsigma}{n} \|\text{diag}(\mathbf{W}_{11})\|, \\ &\leq n^{-1/2+\epsilon}, \end{aligned}$$

where  $\epsilon > 0$  is a small value, with high probability, and in the last step we used the bounds  $\max_{i,j} |\mathbf{W}_{11}(i, j)| \leq 1$  with high probability in (4.51). Indeed, we immediately

have  $\|\text{diag}(\mathbf{W}_{11})\| \leq 1$ . Moreover, by Lemma A.1, we have  $|\text{Sh}_1(2)(i, j)| \prec n^{-1/2}$ ,  $|\text{Sh}_2(2)(i, j)| \prec n^{-1/2}$  and  $p^{-1} \mathbf{y}_i^\top \mathbf{y}_j \prec n^{-1/2}$ . When combined with (4.51), Lemma A.3 leads to  $\|(\text{Sh}_1(2) + \text{Sh}_2(2) - 2f'(2)p^{-1}\mathbf{Y}^\top \mathbf{Y}) \circ \mathbf{W}_{11}\| \leq n^{-1/2+\epsilon}$ . The  $\mathbf{W}_{12}$  can be controlled by (4.49). As a result, we have that with high probability,

$$(4.54) \quad \left\| \frac{1}{n} \mathbf{W} - \frac{1}{n} \mathbf{W}_{a_1} \right\| \leq n^{-1/2+\epsilon}.$$

Since the bulk eigenvalues after scaling are too small, the bound of order  $n^{-1/2+\epsilon}$  is not meaningful. Thus, with the fact that  $\mathbf{W}_{11}$  is at most rank  $m_0 = C_0 \log n$  and the associated eigenvalues might be larger than  $n^{-1/2+\epsilon}$ , we conclude the proof for the case  $\alpha = 1$ . We remark that this is the reason we need the local law via the Stieljes transform to obtain a better estimate for the bulk eigenvalues.

**Case II:**  $1 < \alpha \leq 2$ . It is easy to see that in this case, (4.43) still holds true with high probability. Since  $\beta$  diverges in this case, we find that

$$\frac{t_0^m}{m!} \|\tilde{\mathbf{H}}_m(\mathbf{y})\|_2^2 \leq C n^{C_1 \beta + 1} (m)^{-m-1/2} e^m (C \log n)^m = C n^{C_1 \beta + 1} m^{-1/2} \left( \frac{e C \log n}{m} \right)^m.$$

Now for some fixed large constant  $C_0 > 0$ , we set  $m = C_0 n^{\alpha-1}$ . By a discussion similar to (4.48), we have that for some constants  $C, C_1 > 0$ , with high probability

$$\sum_{m=m_0}^{\infty} \frac{t_0^m}{m!} \|\tilde{\mathbf{H}}_m(\mathbf{y})\|_2^2 \leq C n^{C_1(1-\alpha)n^{\alpha-1}}.$$

The rest of the proof is similar to the case  $\alpha = 1$  except that we can follow (3.9) to show that  $\|\mathbf{W}_1\| \prec n^\delta$  for  $\delta > (3 - \alpha)/2$  and consequently, (4.53) will be updated to

$$\frac{1}{n} \|(\text{Sh}_1 + \text{Sh}_2 - 2f'(\tau)p^{-1}\mathbf{Y}^\top \mathbf{Y} + \varsigma \mathbf{I}_n) \circ \mathbf{W}_{11}\| \prec n^{-\alpha/2}.$$

This completes the proof of (2.22).

**Local law for  $1 \leq \alpha \leq 2$ :** Next, we prove (2.23). Due to similarity, we only focus on the discussion of (2.23); that is, when  $\alpha = 1$ . Recall (2.9). Then we have that

$$(4.55) \quad \mathbf{W} - \mathbf{W}_{a_2} = \mathbf{W}_1 \circ \mathbf{R}_1 + \mathbf{W}_1 \circ (\exp(-2v)\mathbf{1}\mathbf{1}^\top) := \mathbf{E}_1 + \mathbf{E}_2,$$

where  $\mathbf{R}_1$  is the error of the first order entrywise expansion of  $\mathbf{W}_y$  which is defined as

$$\mathbf{R}_1 := \mathbf{W}_y - \left[ \exp(-2v)\mathbf{1}\mathbf{1}^\top + \frac{2v \exp(-2v)}{p} \mathbf{Y}^\top \mathbf{Y} + 2v \exp(-4v) \mathbf{I} \right].$$

Take the same decomposition in (4.46) with some fixed large constant  $C_0 > 0$  and  $m = C_0 \log n$ . By (4.48), we have that with high probability

$$(4.56) \quad \text{rank}(\mathbf{W}_{1,1}) \leq m, \quad \max_{i,j} |\mathbf{W}_{1,2}(i, j)| \leq n^{-D},$$

for some large constant  $D > 2$ .

**Control of  $\mathbf{E}_2$  in (4.55):** Using (4.45) and the fact that  $\mathbf{W}_1 \circ (\exp(-2v)\mathbf{1}\mathbf{1}^\top) = \exp(-2v)\mathbf{W}_1$ , we obtain that

$$(4.57) \quad \mathbf{E}_2 = \exp(-2v)\mathbf{W}_{1,1} + \exp(-2v)\mathbf{W}_{1,2} =: \mathbf{E}_{2,1} + \mathbf{E}_{2,2}.$$

By (4.56) and Lemma A.3, with high probability, for some constant  $C > 0$ , we have

$$(4.58) \quad \text{rank}(\mathbf{E}_{2,1}) \leq m, \quad \|\mathbf{E}_{2,2}\| \leq C n^{-D+1}$$

We control  $m_{\mathbf{W}_{a_2} + \mathbf{E}_1 + \mathbf{E}_2}(z) - m_{\mathbf{W}_{a_2} + \mathbf{E}_1}(z)$  by the triangle inequality,

$$\begin{aligned} |m_{\mathbf{W}_{a_2} + \mathbf{E}_1 + \mathbf{E}_2}(z) - m_{\mathbf{W}_{a_2} + \mathbf{E}_1}(z)| &\leq |m_{\mathbf{W}_{a_2} + \mathbf{E}_1 + \mathbf{E}_2}(z) - m_{\mathbf{W}_{a_2} + \mathbf{E}_1 + \mathbf{E}_{21}}(z)| \\ &\quad + |m_{\mathbf{W}_{a_2} + \mathbf{E}_1 + \mathbf{E}_{21}}(z) - m_{\mathbf{W}_{a_2} + \mathbf{E}_1}(z)|. \end{aligned}$$

By Lemma A.4, we have

$$\begin{aligned} (4.59) \quad &|m_{\mathbf{W}_{a_2} + \mathbf{E}_1 + \mathbf{E}_2}(z) - m_{\mathbf{W}_{a_2} + \mathbf{E}_1 + \mathbf{E}_{2,1}}(z)| \\ &\leq \frac{\text{rank}(\mathbf{E}_{2,2})}{n} \min \left\{ \frac{2}{\eta}, \frac{\|\mathbf{E}_{2,2}\|}{\eta^2} \right\} \leq \frac{C}{n^{D-1}\eta^2}, \end{aligned}$$

where we use the fact that the rank of  $\mathbf{E}_{2,2}$  may be full and  $D$  is large. Similarly, we have

$$\begin{aligned} (4.60) \quad &|m_{\mathbf{W}_{a_2} + \mathbf{E}_{2,1} + \mathbf{E}_1}(z) - m_{\mathbf{W}_{a_2} + \mathbf{E}_1}(z)| \\ &\leq \frac{\text{rank}(\mathbf{E}_{2,1})}{n} \min \left\{ \frac{2}{\eta}, \frac{\|\mathbf{E}_{2,1}\|}{\eta^2} \right\} \leq \frac{2C_0 \log n}{n\eta}, \end{aligned}$$

where we use the fact that  $\|\mathbf{E}_{2,1}\| \leq \|\exp(-2v)\mathbf{W}_1\| \leq \exp(-2v)n^{-\delta}$  for some  $0 < \delta < 1/2$  in the argument leading to (3.9). In conclusion, since  $D$  is a big constant, we control the  $\mathbf{E}_2$  term in the Stieltjes transform, and obtain

$$(4.61) \quad |m_{\mathbf{W}_{a_2} + \mathbf{E}_1 + \mathbf{E}_2}(z) - m_{\mathbf{W}_{a_2} + \mathbf{E}_1}(z)| \leq \frac{3C_0 \log n}{n\eta}$$

for  $z \in \mathcal{D}$  defined in (2.24). It is easy to see that the above control is negligible compared to the rate  $n^{-1/2+\epsilon}\eta^{-2}$  for any arbitrarily small  $\epsilon > 0$ . Consequently, it suffices to focus on  $\mathbf{E}_1$  in (4.55). To control  $\mathbf{E}_1$  in (4.55), note that

$$(4.62) \quad \mathbf{E}_1 = \mathbf{W}_{1,1} \circ \mathbf{R}_1 + \mathbf{W}_{1,2} \circ \mathbf{R}_1$$

and we control

$$\begin{aligned} |m_{\mathbf{W}_{a_2} + \mathbf{E}_1}(z) - m_{\mathbf{W}_{a_2}}(z)| &\leq |m_{\mathbf{W}_{a_2} + \mathbf{W}_{1,1} \circ \mathbf{R}_1 + \mathbf{W}_{1,2} \circ \mathbf{R}_1}(z) - m_{\mathbf{W}_{a_2} + \mathbf{W}_{1,1} \circ \mathbf{R}_1}(z)| \\ &\quad + |m_{\mathbf{W}_{a_2} + \mathbf{W}_{1,1} \circ \mathbf{R}_1}(z) - m_{\mathbf{W}_{a_2}}(z)|. \end{aligned}$$

By a discussion similar to (4.13) with for the cloud points  $\{\mathbf{y}_i\}$  (or see the proof of Lemma 4.2 of Ding and Wu (2020)), we have

$$(4.63) \quad \max_{i,j} |\mathbf{R}_1(i,j)| \prec n^{-1/2}.$$

Together with (4.56), by Lemma A.3, we conclude that

$$(4.64) \quad \|\mathbf{W}_{1,2} \circ \mathbf{R}_1\| \prec n^{-D+1/2}.$$

This error is negligible since  $D > 2$  by the same argument as (4.59), thus we have the control for  $|m_{\mathbf{W}_{a_2} + \mathbf{W}_{1,1} \circ \mathbf{R}_1 + \mathbf{W}_{1,2} \circ \mathbf{R}_1}(z) - m_{\mathbf{W}_{a_2} + \mathbf{W}_{1,1} \circ \mathbf{R}_1}(z)|$ . The rest of the proof leaves to control  $|m_{\mathbf{W}_{a_2} + \mathbf{W}_{1,1} \circ \mathbf{R}_1}(z) - m_{\mathbf{W}_{a_2}}(z)|$ . Set  $\mathcal{E}_1 := \mathbf{W}_{1,1} \circ \mathbf{R}_1$  for convenience. Note that with high probability, for some constant  $C > 0$ , we have that

$$(4.65) \quad \max_{i,j} |\mathbf{W}_{1,1}(i,j)| \leq C.$$

By the definition of Stieltjes transform, for any even integer  $q$ , we have

$$|m_{\mathbf{W}_{a_2} + \mathcal{E}_1}(z) - m_{\mathbf{W}_{a_2} + \mathbf{R}_1}(z)|^q \leq \left( \frac{1}{n} \sum_{i=1}^n \frac{|\lambda_i(\mathbf{W}_{a_2} + \mathcal{E}_1) - \lambda_i(\mathbf{W}_{a_2} + \mathbf{R}_1)|}{|\lambda_i(\mathbf{W}_{a_2} + \mathcal{E}_1) - z| |\lambda_i(\mathbf{W}_{a_2} + \mathbf{R}_1) - z|} \right)^q,$$

which, by the Cauchy-Schwarz inequality, is bounded by

$$\begin{aligned}
& \frac{1}{n^q} \left[ \left( \sum_{i=1}^n |\lambda_i(\mathbf{W}_{a_2} + \mathcal{E}_1) - \lambda_i(\mathbf{W}_{a_2} + \mathbf{R}_1)|^2 \right) \right. \\
& \quad \times \left. \left( \sum_{i=1}^n \frac{1}{|\lambda_i(\mathbf{W}_{a_2} + \mathcal{E}_1) - z|^2 |\lambda_i(\mathbf{W}_{a_2} + \mathbf{R}_1) - z|^2} \right) \right]^{q/2} \\
(4.66) \quad & \leq \frac{1}{n^{q/2} \eta^{2q}} (\text{tr}\{(\mathcal{E}_1 - \mathbf{R}_1)^2\})^{q/2},
\end{aligned}$$

where the last inequality comes from the Hoffman-Wielandt inequality (Lemma A.4) and the trivial bound  $|\lambda - z|^{-1} \leq \eta^{-1}$  for any  $\lambda \in \mathbb{R}$ . The rest of the proof leaves to control the right-hand side of (4.66). By (4.65) and the fact that  $\mathcal{E}_1 - \mathbf{R}_1 = (\mathbf{W}_{1,1} - \mathbf{1}\mathbf{1}^\top) \circ \mathbf{R}_1$ . Hence, since  $\mathcal{E}$  is symmetric, for some constant  $C > 0$ , we can replace (4.66) with

$$(4.67) \quad \frac{C}{n^{q/2} \eta^{2q}} [\text{tr}(\mathbf{R}_1^2)]^{q/2}.$$

Thus, we only need to consider the  $\mathbf{R}_1$  part, and we claim that (4.67) can be controlled by a term of order  $(\log n)^q n^{-q/2} \eta^{-2q}$ , where the proof can be found in (Ding and Wu, 2020, eq. (C.8)). To finish the proof, by the same argument of controlling  $|m_{\mathbf{W}_{a_2} + \mathcal{E}_1}(z) - m_{\mathbf{W}_{a_2} + \mathbf{R}_1}(z)|^q$ , we get  $|m_{\mathbf{W}_{a_2} + \mathbf{R}_1}(z) - m_{\mathbf{W}_{a_2}}(z)|^q$  controlled by a term of order  $(\log n)^q n^{-q/2} \eta^{-2q}$ . By collecting a sequence of controls, including  $|m_{\mathbf{W}_{a_2} + \mathbf{E}_1 + \mathbf{E}_2}(z) - m_{\mathbf{W}_{a_2} + \mathbf{E}_1}(z)|$  and  $|m_{\mathbf{W}_{a_2} + \mathbf{E}_1}(z) - m_{\mathbf{W}_{a_2}}(z)|$ , we conclude the proof.  $\square$

**4.5. Proof of Corollaries 2.9 and 2.10 for transition matrices with  $h = p$ .** In this section, we prove the results for the transition matrix  $\mathbf{A}_x$ .

*Proof of Corollary 2.9.* We then prove Corollary 2.9. First of all, we prove part (2) of the results. By (4.36) and the definition of  $\mathbf{D}$  (e.g.  $\mathbf{D}_{ii} = 1$ ), we find that with probability at least  $1 - O(n^{1-t(\alpha-1)/2})$ , for some constant  $C > 0$ ,

$$\|\mathbf{D} - \mathbf{I}_n\| \leq Cn \exp \left( -v \left( \frac{\lambda}{p} \right)^{1-t} \right).$$

This bound together with (2.20) lead to

$$\|\mathbf{W} - \mathbf{D}^{-1/2} \mathbf{W} \mathbf{D}^{-1/2}\| \leq 2Cn \exp \left( -v \left( \frac{\lambda}{p} \right)^{1-t} \right).$$

Since  $\mathbf{A}$  is similar to  $\mathbf{D}^{-1/2} \mathbf{W} \mathbf{D}^{-1/2}$ , by Weyl's lemma, we conclude the claim. The polynomial case can be dealt with analogously. This concludes the proof for the fast divergent case. Next, we handle part (1). When  $\alpha = 0$ , it follows from the fact that

$$(4.68) \quad \|(n^{-1} \mathbf{D})^{-1} - f(2)^{-1} \mathbf{I}_n\| \prec n^{-1/2}.$$

The proof can be found in (Ding and Wu, 2020, Lemma 4.5), and we omit it. By a standard perturbation argument, we have that when  $n$  is sufficiently large,

$$|\lambda_i(n \mathbf{D}^{-1/2} \mathbf{W} \mathbf{D}^{-1/2}) - \lambda_i(f(2)^{-1} \mathbf{W})| \prec n^{-1/2}$$

for all  $i$ . When  $0 < \alpha < 1$ , by a discussion similar to (4.68) using Lemma A.2, we find that

$$\|(n^{-1} \mathbf{D})^{-1} - f(\tau)^{-1} \mathbf{I}_n\| \prec n^{-1/2} + \frac{\lambda}{p},$$

and by the same argument as that for  $\alpha = 0$ , we conclude the proof.  $\square$

*Proof of Corollary 2.10.* We start with the first statement. Note that

$$(4.69) \quad \begin{aligned} \|\mathbf{A} - \mathbf{A}_{a_1}\| &\leq \|\mathbf{D}^{-1}(\mathbf{W} - \mathbf{W}_{a_1})\| + \|\mathbf{D}^{-1}(\mathbf{D}_{a_1} - \mathbf{D})\mathbf{D}_{a_1}^{-1}\mathbf{W}_{a_1}\| \\ &\leq \|\mathbf{D}^{-1}\| \|\mathbf{W} - \mathbf{W}_{a_1}\| + \|\mathbf{D}^{-1}\| \|\mathbf{D} - \mathbf{D}_{a_1}\| \|\mathbf{D}_{a_1}^{-1}\mathbf{W}_{a_1}\|. \end{aligned}$$

The first term can be easily bounded by  $\|\mathbf{W} - \mathbf{W}_{a_1}\|$  due to the trivial bound  $\|\mathbf{D}\| \geq 1$ . For the second term, note that  $\|\mathbf{D}_{a_1}^{-1}\mathbf{W}_{a_1}\| \leq 1$  since it is a transition matrix. Since  $\mathbf{D}$  and  $\mathbf{D}_{a_1}$  are both diagonal, we control  $|\mathbf{D}(i, i) - \mathbf{D}_{a_1}(i, i)|$ . By a direct expansion, we have

$$(4.70) \quad \begin{aligned} \mathbf{D}(i, i) - \mathbf{D}_{a_1}(i, i) &= \sum_{j \neq i} \exp\left(-v \frac{\|\mathbf{x}_i - \mathbf{x}_j\|_2^2}{p}\right) - \sum_{j \neq i} \exp(-2v) \exp\left(-v \frac{(\mathbf{x}_{i1} - \mathbf{x}_{j1})^2}{p}\right) \\ &= \sum_{j \neq i} \exp\left(-v \frac{(\mathbf{x}_{i1} - \mathbf{x}_{j1})^2}{p}\right) \left[ \exp\left(-v \frac{\|\mathbf{y}_i - \mathbf{y}_j\|_2^2}{p}\right) - \exp(-2v) \right]. \end{aligned}$$

Using (3.16), we find that with high probability, there exists  $O(n^\delta)$ ,  $0 < \delta < 1$ , amount of  $\mathbf{y}_{i1}$ 's such that  $|\mathbf{y}_{i1}| \leq n^{-(1-\delta)}$ . Moreover, since  $f(2)$  is the zero-th order Taylor expansion for  $f(\|\mathbf{y}_i - \mathbf{y}_j\|/p)$  at 2, it is easy to see that

$$(4.71) \quad \left| \exp\left(-v \frac{\|\mathbf{y}_i - \mathbf{y}_j\|_2^2}{p}\right) - \exp(-2v) \right| \prec \frac{1}{\sqrt{p}}.$$

Combine the above results, we obtain that for some constant  $C > 0$ , by setting

$$(4.72) \quad \begin{aligned} |\mathbf{D}(i, i) - \mathbf{D}_{a_1}(i, i)| &\prec n^\delta \max_j \left[ \exp\left(-v \frac{\|\mathbf{y}_i - \mathbf{y}_j\|_2^2}{p}\right) - \exp(-2v) \right] \\ &\quad + (n-1 - Cn^\delta) \exp(-vp^{\alpha-1}n^{-2(1-\delta)}) \\ &\prec n^{\delta-1/2} + n \exp(-vn^{\alpha+2\delta-3}). \end{aligned}$$

By choosing  $\delta < \frac{1}{2}$  and  $\delta > \frac{3-\alpha}{2}$ , which is always feasible since  $\alpha > 2$ , we can show that

$$|\mathbf{D}(i, i) - \mathbf{D}_{a_1}(i, i)| \prec n^{\frac{2-\alpha}{2}}.$$

This finishes the proof for the first statement.

For the second statement, we focus our discussion on the case when  $\alpha = 1$ . Note that

$$\mathbf{D}(i, i) = \sum_{j \neq i} \exp\left(-v \frac{\lambda(\mathbf{y}_{i1} - \mathbf{y}_{j1})^2}{p}\right) \exp\left(-v \frac{\|\mathbf{y}_i - \mathbf{y}_j\|_2^2}{p}\right).$$

Since  $f(2) \asymp 1$ , by (4.71), we find that for some constant  $C > 0$ , with high probability, we have that when  $n$  is large enough

$$\mathbf{D}(i, i) \geq C \sum_{j \neq i} \exp\left(-v \frac{\lambda(\mathbf{y}_{i1} - \mathbf{y}_{j1})^2}{p}\right).$$

Again by (3.16), with high probability, for some constant  $C > 0$  and any small constant  $\epsilon > 0$ , since  $\alpha = 1$ , i.e.,  $\lambda \asymp p$ , we have

$$\mathbf{D}(i, i) \geq Cn^{1-\epsilon}.$$

This implies that  $\|\mathbf{D}^{-1}\| \prec n^{-1}$ , where the  $n^\epsilon$  factor can be absorbed into the stochastic dominance. Combining with (4.69), we find that

$$\|\mathbf{A} - \mathbf{A}_{a_1}\| \prec \left\| \frac{1}{n} \mathbf{W} - \frac{1}{n} \mathbf{W}_{a_1} \right\| + \frac{1}{n} \|\mathbf{D} - \mathbf{D}_{a_1}\|,$$

where we again used the fact that  $\|\mathbf{D}_{a_1}^{-1} \mathbf{W}_{a_1}\| \leq 1$ . To prove a similar result like (2.22), we need to control the second term of the right-hand side of the above equation. By (4.70) and (4.71), we immediately see that

$$\frac{1}{n} \|\mathbf{D} - \mathbf{D}_{a_1}\| \prec n^{-1/2}.$$

This concludes our proof for the counterpart of (2.22) for the case  $\alpha = 1$ .

When  $1 < \alpha \leq 2$ , the only difference is that using (4.70), (4.71) and (4.72), we show that

$$\frac{1}{n} \|\mathbf{D} - \mathbf{D}_{a_1}\| \prec n^{-\alpha/2}.$$

This completes the discussion of the first part of the second statement.

For the counterpart of (2.23), when  $\alpha = 1$ , using the definition (4.55), we decompose

$$\mathbf{D}^{-1} \mathbf{W} - \mathbf{D}_{a_3}^{-1} \mathbf{W}_{a_3} = \mathbf{D}^{-1} \mathbf{E}_1 + \mathbf{D}^{-1} (\mathbf{D}_{a_3} - \mathbf{D}) \mathbf{D}_{a_3}^{-1} \mathbf{W}_{a_3} := \mathbf{S}_1 + \mathbf{S}_2.$$

Note that  $m_{\mathbf{A}} = m_{\mathbf{A}_{a_3} + \mathbf{S}_1 + \mathbf{S}_2}$ . By the second inequality of Lemma A.4, we have that

$$|m_{\mathbf{A}_{a_3} + \mathbf{S}_1 + \mathbf{S}_2} - m_{\mathbf{A}_{a_3} + \mathbf{S}_2}| \leq \frac{\|\mathbf{S}_1\|}{n^2}.$$

By (4.63) with Lemma 3.5 and the obtained result  $\|\mathbf{D}^{-1}\| \prec n^{-1}$ , we conclude that  $\|\mathbf{S}_1\| \prec n^{-1/2}$ , which leads to

$$|m_{\mathbf{A}_{a_3} + \mathbf{S}_1 + \mathbf{S}_2} - m_{\mathbf{A}_{a_3} + \mathbf{S}_2}| \prec \frac{1}{\sqrt{n\eta^2}}.$$

It remains to study  $\mathbf{S}_2$ . Observe that

$$\mathbf{D}_{a_3}(i, i) - \mathbf{D}(i, i) = \sum_{j \neq i} \mathbf{W}_1(i, j) (-\mathbf{R}_1(i, j)).$$

Again by (4.63) with Lemma 3.5 and the obtained result  $\|\mathbf{D}^{-1}\| \prec n^{-1}$ , together with the fact that  $\|\mathbf{D}_{a_3}^{-1} \mathbf{W}_{a_3}\| \prec 1$ , we conclude that  $\|\mathbf{S}_2\| \prec n^{-1/2}$ , which by Lemma A.4 yields that

$$\|m_{\mathbf{A}_{a_3} + \mathbf{S}_2} - m_{\mathbf{A}_{a_3}}\| \prec \frac{1}{\sqrt{n\eta^2}}.$$

This proves the case for  $\alpha = 1$ . The case  $1 < \alpha \leq 2$  are analogous and we omit the details here.  $\square$

**4.6. Proof of Theorem 2.11, results with the adaptive bandwidth.** In this section, we prove Theorem 2.11. We focus our discussion on  $\mathbf{W}$ .

*Proof.* For the first statement, it is easy to see that it follows from the claims that

$$(4.73) \quad h \asymp p,$$

holds with high probability. In fact, under the assumption of (4.73), we can rewrite

$$f\left(\frac{\|\mathbf{x}_i - \mathbf{x}_j\|_2^2}{h}\right) = g\left(\frac{\|\mathbf{x}_i - \mathbf{x}_j\|_2^2}{p}\right),$$

where  $g(x) := f(px/h)$ . Then we can apply all the proof of Theorems 2.3 and 2.5 to the kernel function  $g(x)$  to conclude the proof. The only difference is that we will get an extra factor  $p/h$  for the derivative and we omit the details. It remains to show that (4.73) holds with high probability. Recall that the summation of independent Sub-Gaussian random variables is also Sub-Gaussian and the square of Sub-Gaussian is Sub-Exponential. Since  $\mathbf{x}_i, \mathbf{x}_j, i \neq j$ , are independent, the random variable  $\|\mathbf{x}_i - \mathbf{x}_j\|^2$  follows a Sub-Exponential distribution, and by Lemma A.2, we have

$$\|\mathbf{x}_i - \mathbf{x}_j\|^2 = 2(p + \lambda) + O_{\prec}(p^\alpha + \sqrt{p}).$$

Since  $\alpha < 1$ , with high probability, when  $p$  is large enough,  $\|\mathbf{x}_i - \mathbf{x}_j\|^2$  is concentrated around  $2p$ . Thus, for any  $\omega \in (0, 1)$ , (4.73) holds with high probability.

We next prove the second statement when  $1 \leq \alpha \leq 2$ . With a discussion similar to (4.73), we claim that when  $\alpha \geq 1$ , for some given sufficiently small  $\epsilon > 0$ , we have that with high probability and some constants  $C_1, C_2 > 0$ ,

$$(4.74) \quad C_1(\lambda n^{-2\epsilon} + p) \leq h \leq C_2 \lambda \log^2 n.$$

In fact, we notice that

$$\begin{aligned} \|\mathbf{x}_i - \mathbf{x}_j\|^2 &= \sum_{k=2}^p (\mathbf{y}_{ik} - \mathbf{y}_{jk})^2 + \lambda(\mathbf{y}_{i1} - \mathbf{y}_{j1})^2 \\ &= 2(p - 1) + O_{\prec}(\sqrt{p}) + \lambda(\mathbf{y}_{i1} - \mathbf{y}_{j1})^2. \end{aligned}$$

On one hand, since  $\mathbf{y}_{i1}$  and  $\mathbf{y}_{j1}$  are Sub-Gaussian, we have that for some constant  $C > 0$   $\lambda(\mathbf{y}_{i1} - \mathbf{y}_{j1})^2 \leq C \lambda \log^2 n$  with high probability; on the other hand, using a discussion similar to (3.16), with high probability, we have that there are at least  $Cn^{1-\epsilon}$   $\mathbf{y}_{k1}$ 's such that  $\lambda(\mathbf{y}_{i1} - \mathbf{y}_{j1})^2 \geq \lambda n^{-2\epsilon}$ . Since  $\omega \in (0, 1)$ , when  $n$  is large enough, we have  $\omega > Cn^{1-\epsilon}/n = Cn^{-\epsilon}$ . This proves (4.74). Denote

$$\kappa \equiv \kappa(\lambda) := \frac{2p}{h}.$$

Recall (2.9) and (2.26). By a discussion similar to (4.31), we can easily see that

$$(4.75) \quad \|\mathbf{W} - \mathbf{W}_{b_1}\| \prec \frac{\sqrt{p}}{h} \|\mathbf{W}_1\|.$$

The argument of the counterpart of (2.22) regarding  $\mathbf{W}_1$  with  $h$  satisfying (4.74) is analogous to the Cases (I) and (II) in the proof of (2.22) with some necessary modifications. The difference is that, due to (4.74), we have that

$$\frac{1}{C_2 \log^2 n} \leq \beta \leq \frac{1}{C_1(n^{-2\epsilon} + p/\lambda)}, \quad \beta = \frac{\lambda}{h}.$$

First, when  $\beta = O(1)$ , the discussion reduces to the Case (I) (i.e., the arguments below (4.42)) of the proof of Theorem 2.8. Second, when  $\beta$  diverges and  $\beta \leq C \min\{n^{2\epsilon}, n^{\alpha-1}\}$  for some constant  $C > 0$ , the discussion reduces to the Case (II) by setting  $m = C_0 n^{\alpha'}$ , where  $\alpha' \leq \min\{2\epsilon, \alpha - 1\}$ . Finally, we discuss  $\beta = o(1)$  satisfying  $\beta \geq 1/(C_2 \log^2 n)$ . In this case, we still have  $t_0 < 1$ . Recall (4.40). However, since  $1 - t_0^2 \asymp \frac{1}{\beta} \leq C \log^2 n$  for some constant  $C > 0$ . However, compared to the error bound in (4.48), the extra factor  $\log^2 n$  is negligible. Then the case still reduces to Case (I). This completes the proof.

To see the counterpart of (2.23), we point out that the argument staring from (4.55) still applies except that (4.63) should be updated to

$$\max_{i,j} |\mathbf{R}_1(i, j)| \prec \frac{\sqrt{p}}{\lambda}.$$

Finally, we prove the third statement. By (4.75) and Lemma A.3 to control  $\lambda_1(\mathbf{W}_1) \prec p$ , we see that

$$\|\mathbf{W} - \mathbf{W}_{b_1}\| \prec \frac{p^{3/2}}{\lambda}.$$

Moreover, recall (2.26), by Lemmas 3.5 and A.3, we have that

$$\|\mathbf{W}_{b_1} - \mathbf{W}_1\| \prec \frac{p^2}{\lambda},$$

where we used  $f(\kappa) \asymp 1 + p/h$  and (4.74). This completes our proof.  $\square$

## 5. DISCUSSION

We focus on the GL with the exponential-type kernel that is constructed from the high dimensional noisy dataset, which is the basic quantity in several unsupervised learning algorithms. The analysis shed a light on exploring the spectral distribution of GL under other setups. For example, the locally linear embedding (LLE) (Roweis and Saul, 2000), vector diffusion map (VDM) (Singer and Wu, 2012), among others, are all kernel-based unsupervised algorithms based on GL, where the kernel is involved explicitly or implicitly in one or another form. For example, from the LLE algorithm, it is not clear how the kernel is involved without a proper transform (Wu and Wu, 2018). Moreover, the associated kernel is adaptive to data and not symmetric. In VDM, the affinity matrix is no longer scalar-valued, but group-valued, so that more local geometric relationship among cloud points can be captured. Clearly, in practice we may encounter different kernels, and it is interesting future work to analyze these GL's. In this subsection, we briefly discuss the challenge to handle more general kernels. As is indicated above, the developed results when the signal strength is in the bounded and slowly divergent regimes can be generalized to more general kernels with mild conditions. However, it is no longer the case when the kernel is not of exponential type. Take the kernel of polynomial type into account, for example,  $f(x) = (1 + x)^{-v}$ , where  $v > 0$ . In this case, if we write

$$(5.1) \quad \|\mathbf{x}_i - \mathbf{x}_j\|_2^2 = \lambda(\mathbf{y}_{i1} - \mathbf{y}_{j1})^2 + \|\mathbf{y}_i - \mathbf{y}_j\|_2^2 := S_{ij} + N_{ij},$$

we have that

$$(5.2) \quad \mathbf{W}(i, j) = \left(1 + \frac{S_{ij}}{p} + \frac{N_{ij}}{p}\right)^{-v} = \left(1 + \frac{N_{ij}}{p}\right)^{-v} \left(1 + \frac{S_{ij}}{p + N_{ij}}\right)^{-v}.$$

Thus, the “signal part” of  $\mathbf{W}$ , also denoted as  $\mathbf{W}_1$ , is

$$\mathbf{W}_1(i, j) = \left(1 + \frac{S_{ij}}{p + N_{ij}}\right)^{-v},$$

and the counterpart  $\mathbf{W}_y$  is  $\left(1 + \frac{N_{ij}}{p}\right)^{-v}$ . Note that  $\mathbf{W}_1$  is not purely from the signal, but also has the noise part involved. When the signal is very strong, like  $\alpha > 2$ , clearly we have  $S_{ij} \gg p + N_{ij}$  with high probability, and hence  $\mathbf{W}_1$  is more like the one purely from the signal. Consequently, we still have a relation

$$(5.3) \quad \mathbf{W} = \mathbf{W}_y \circ \mathbf{W}_1.$$

With this “decomposition”, we can derive some special cases easily. For example, for any given constant  $t \in (0, 1)$ , if

$$(5.4) \quad \alpha > \max \left\{ \frac{2}{t} + 1, \frac{1}{v(1-t)} + 1 \right\},$$

then we can easily obtain that with probability at least  $1 - O(n^{1-t(\alpha-1)/2})$ , for some constant  $C > 0$  and all  $1 \leq i \leq n$ ,

$$(5.5) \quad |\lambda_i(\mathbf{W}) - 1| \leq Cn^{-v(\alpha-1)(1-t)+1}.$$

The proof is similar to the exponential decay case, except for (4.37). In fact, since we have

$$\mathbf{W}(i, j) = \left(1 + \frac{\lambda \|\mathbf{x}_i - \mathbf{x}_j\|_2^2}{p \lambda}\right)^{-v},$$

by (4.35) and under the assumption of (5.4), we have that with probability at least  $1 - O(n^{1-t(\alpha-1)/2})$ , for some constant  $C > 0$ , we have that

$$\left| \sum_{j \neq i} \mathbf{W}(i, j) \right| \leq Cn \left( \frac{\lambda}{p} \left( \frac{p}{\lambda} \right)^t \right)^{-v} = Cn \left( \frac{\lambda}{p} \right)^{-v(1-t)}.$$

Consequently, by Lemma A.3, we have that for all  $1 \leq i \leq n$ ,

$$(5.6) \quad \|\lambda_i(\mathbf{W}) - 1\| \leq Cn \left( \frac{\lambda}{p} \right)^{-v(1-t)}.$$

We need the second part of (5.4) since we request the right-hand side of (5.6) to be small. This concludes our proof.

However, the situation becomes more complicated when the signal strength is in the moderately divergent regime or the fast divergent regime but (5.4) is not satisfied. In this case, a generalization of the Mehler's formula is less convenient, and a different analysis technique is needed, especially, the decomposition (5.2) will be insufficient since the signal part  $S_{ij}$  will not dominate the noise part  $p + N_{ij}$  in an adequate way.

## REFERENCES

BAIK, J., BEN AROUS, G. and PÉCHÉ, S. (2005). Phase transition of the largest eigenvalue for nonnull complex sample covariance matrices. *Ann. Probab.* **33** 1643–1697.

BAO, Z., DING, X., WANG, J. and WANG, K. (2020). Statistical inference for principal components of spiked covariance matrix. *arXiv preprint arXiv 2008.11903*.

BELKIN, M. and NIYOGI, P. (2003). Laplacian Eigenmaps for Dimensionality Reduction and Data Representation. *Neural. Comput.* **15** 1373–1396.

BÉRARD, P., BESSON, G. and GALLOT, S. (1994). Embedding Riemannian manifolds by their heat kernel. *Geometric & Functional Analysis GAFA* **4** 373–398.

BLOEMENDAL, A., KNOWLES, A., YAU, H.-T. and YIN, J. (2016). On the principal components of sample covariance matrices. *Probab. Theory Related Fields* **164** 459–552.

CHENG, X. and SINGER, A. (2013). The spectrum of random inner-product kernel matrices. *Random Matrices: Theory and Applications* **2** 1350010.

COIFMAN, R. R. and LAFON, S. (2006). Diffusion maps. *Applied and Computational Harmonic Analysis* **21** 5–30.

DING, X. and WU, H.-T. (2020). On the spectral property of kernel-based sensor fusion algorithms of high dimensional data. *IEEE Transactions on Information Theory (in press)*.

DING, X. and YANG, F. (2020). Spiked separable covariance matrices and principal components. *The Annals of Statistics (in press)*.

DO, Y. and VU, V. (2013). The spectrum of random kernel matrices: universality results for rough and varying kernels. *Random Matrices: Theory and Applications* **2** 1350005.

DUNSON, D. B., WU, H.-T. and WU, N. (2019). Diffusion based Gaussian process regression via heat kernel reconstruction. *arXiv preprint arXiv:1912.05680*.

EL KAROUI, N. (2010a). On information plus noise kernel random matrices. *Ann. Statist.* **38** 3191–3216.

EL KAROUI, N. (2010b). The spectrum of kernel random matrices. *Ann. Statist.* **38** 1–50.

EL KAROUI, N. and WU, H.-T. (2015). Graph connection Laplacian and random matrices with random blocks. *Information and Inference: A Journal of the IMA* **4** 1–44.

EL KAROUI, N. and WU, H.-T. (2016). Graph connection Laplacian methods can be made robust to noise. *The Annals of Statistics* **44** 346–372.

ERDŐS, L., KNOWLES, A. and YAU, H.-T. (2013). Averaging fluctuations in resolvents of random band matrices. *Ann. Henri Poincaré* **14** 1837–1926.

FAN, Z. and MONTANARI, A. (2019). The spectral norm of random inner-product kernel matrices. *Probability Theory and Related Fields* **173** 27–85.

FOATA, D. (1978). A combinatorial proof of the mehler formula. *Journal of Combinatorial Theory, Series A* **24** 367 – 376.

HORN, R. and JOHNSON, C. (2012). *Matrix Analysis*. 2nd ed. Cambridge University Press.

JOHNSTONE, I. M. (2001). On the distribution of the largest eigenvalue in principal components analysis. *Ann. Statist.* **29** 295–327.

KNOWLES, A. and YIN, J. (2017). Anisotropic local laws for random matrices. *Probability Theory and Related Fields* **169** 257–352.

MARCHENKO, V. A. and PASTUR, L. A. (1967). Distribution of eigenvalues for some sets of random matrices. *Mathematics of the USSR-Sbornik* **1** 457–483.

NGO, H. Q. (2002).  $\mathbb{P}$ -Species and the q-Mehler formula. *Sém. Lothar. Combin* B48b.

PASSEMIER, D. and YAO, J. (2014). Estimation of the number of spikes, possibly equal, in the high-dimensional case. *Journal of Multivariate Analysis* **127** 173–183.

PAUL, D. (2007). Asymptotics of sample eigenstructure for a large dimensional spiked covariance model. *Statistica Sinica* **17** 1617–1642.

ROWEIS, S. T. and SAUL, L. K. (2000). Nonlinear dimensionality reduction by locally linear embedding. *Science* **290** 2323–2326.

SHEN, C. and WU, H.-T. (2020). Scalability and robustness of spectral embedding: landmark diffusion is all you need. *arXiv preprint arXiv:2001.00801*.

SINGER, A. and WU, H.-T. (2012). Vector diffusion maps and the connection Laplacian. *Comm. Pure Appl. Math.* **65** 1067–1144.

VERSHTYNIN, R. (2018). *High-Dimensional Probability: An Introduction with Applications in Data Science*. Cambridge Series in Statistical and Probabilistic Mathematics, Cambridge University Press.

WU, H.-T. and WU, N. (2018). Think globally, fit locally under the Manifold Setup: Asymptotic Analysis of Locally Linear Embedding. *Annals of Statistics* **46** 3805–3837.

#### APPENDIX A. AUXILIARY LEMMAS

In this section, we record some auxiliary lemmas for our technical proof. We start with the concentration inequalities for the sub-Gaussian random vectors satisfying (1.2). The first lemma establishes the concentration inequalities when  $\lambda$  is bounded.

**Lemma A.1.** Suppose (1.1), (1.2) and (1.3) hold. We further assume that  $\lambda \asymp 1$ . Then, for  $i \neq j$  and  $t > 0$ , we have

$$(A.1) \quad \mathbb{P} \left( \left| \frac{1}{p} \mathbf{y}_i^\top \mathbf{y}_j \right| > t \right) \leq \exp(-pt^2/2),$$

as well as

$$(A.2) \quad \mathbb{P} \left( \left| \frac{1}{p} \mathbf{x}_i^\top \mathbf{x}_j - \frac{\lambda}{p} \mathbf{y}_{i1} \mathbf{y}_{j1} \right| > t \right) \leq \exp(-pt^2/2).$$

Moreover, for the diagonal items, for  $t > 0$ , we have for some universal constants  $C, C_1 > 0$ ,

$$(A.3) \quad \mathbb{P} \left( \left| \frac{1}{p} \|\mathbf{y}_i\|_2^2 - 1 \right| > t \right) \leq \begin{cases} 2 \exp(-C_1 pt^2), & 0 < t \leq C; \\ 2 \exp(-C_1 pt), & t > C. \end{cases}$$

as well as

$$(A.4) \quad \mathbb{P} \left( \left| \frac{1}{p} \|\mathbf{x}_i\|_2^2 - \frac{\lambda}{p} \mathbf{y}_{i1}^2 \right| > t \right) \leq \begin{cases} 2 \exp(-C_1 pt^2), & 0 < t \leq C; \\ 2 \exp(-C_1 pt), & t > C. \end{cases}$$

Especially, the above results imply that

$$(A.5) \quad \frac{1}{p} |\mathbf{y}_i^\top \mathbf{y}_j| \prec n^{-1/2}, \quad \frac{1}{p} |\mathbf{x}_i^\top \mathbf{x}_j| \prec n^{-1/2}.$$

as well as

$$(A.6) \quad \left| \frac{1}{p} \|\mathbf{y}_i\|_2^2 - 1 \right| \prec n^{-1/2}, \quad \left| \frac{1}{p} \|\mathbf{x}_i\|_2^2 - \left( 1 + \frac{\lambda}{p} \right) \right| \prec n^{-1/2}.$$

*Proof.* For  $i \neq j$ , (A.1) has been proved in (Ding and Wu, 2020, Lemma A.2). (A.2) follows from the fact that  $\mathbf{x}_i^\top \mathbf{x}_j - \mathbf{y}_i^\top \mathbf{y}_j = (\lambda/p) \mathbf{y}_{i1} \mathbf{y}_{j1}$ . (A.5) follows from (A.1) and (A.2) for scalar random variables and the fact  $\lambda < \infty$ .

For  $i = j$ , (A.3) has been proved in (Vershynin, 2018, Corollary 2.8.3). (A.4) follows from the fact that  $\|\mathbf{x}_i\|_2^2 - \|\mathbf{y}_i\|_2^2 = (\lambda/p) \mathbf{y}_{i1}^2$ . (A.6) follows from (A.4), (A.3) for scalar random variables and the fact  $\lambda < \infty$ .  $\square$

Then we provide the concentration inequalities when  $\lambda$  is in the slowly divergent regime. Indeed, in this regime, the results of the diagonal parts of Lemma A.1 still apply.

**Lemma A.2.** Suppose (1.1), (1.3) and (1.2) hold. We further assume that  $\lambda = n^\alpha$ , where  $0 < \alpha < 1$ . Then when  $i \neq j$ , we have

$$(A.7) \quad \frac{1}{p} |\mathbf{x}_i^\top \mathbf{x}_j| \prec \frac{\lambda}{n} + \frac{1}{\sqrt{n}}, \quad \left| \frac{1}{p} \|\mathbf{x}_i\|_2^2 - \left( 1 + \frac{\lambda}{p} \right) \right| \prec \frac{\lambda}{n} + \frac{1}{\sqrt{n}}.$$

*Proof.* We only discuss the second term and the first item can be dealt with in a similar way. We define  $\lambda_f = \lfloor \lambda \rfloor$  as the floor of  $\lambda$ . Note that we have

$$(A.8) \quad \frac{\lambda_f}{p} \mathbf{y}_{i1}^2 + \frac{1}{p} \sum_{j=2}^p \mathbf{y}_{ij}^2 \leq \frac{1}{p} \|\mathbf{x}_i\|_2^2 \leq \frac{\lambda_f + 1}{p} \mathbf{y}_{i1}^2 + \frac{1}{p} \sum_{j=2}^p \mathbf{y}_{ij}^2.$$

Without loss of generality, we assume that  $\sqrt{\lambda_f}$  is some integer. Note that we can decompose

$$\sqrt{\lambda_f} \mathbf{y}_{i1} = \sum_{k=1}^{\sqrt{\lambda_f}} z_k,$$

where  $\{z_k\}$  is a sequence of i.i.d. sub-Gaussian random variables independent of  $\{\mathbf{y}_{ij}\}_{j \geq 2}$ . Hence, to bound the right-hand side of (A.8), we need to control

$$\frac{1}{p} \left[ \left( \sum_{k=1}^{\sqrt{\lambda_f}} z_k \right)^2 + \sum_{j=1}^p \mathbf{y}_{ij}^2 \right] = \frac{1}{p} \sum_{k=1}^{p+\sqrt{\lambda_f}} z_k^2 + \frac{1}{p} \sum_{k_1 \neq k_2} z_{k_1} z_{k_2},$$

where we use the convention that  $z_{k+\sqrt{\lambda_f}} = \mathbf{y}_{ik}$ . By Lemma A.1, we have that

$$\left| \frac{1}{p} \sum_{k=1}^{p+\sqrt{\lambda_f}} z_k^2 - \left( 1 + \frac{\sqrt{\lambda_f}}{p} \right) \right| = \frac{p + \sqrt{\lambda_f}}{p} \left| \frac{1}{p + \sqrt{\lambda_f}} \sum_{k=1}^{p+\sqrt{\lambda_f}} z_k^2 - 1 \right| \prec n^{-1/2},$$

where we use the fact that  $(p + \sqrt{\lambda_f})/p \asymp 1$  by the assumption that  $\alpha < 1$ . Next, for any given large but finite even integer  $q$ , we see that for some constant  $C = C(q) > 0$ ,

$$\mathbb{E} \left| \frac{1}{p} \sum_{k_1 \neq k_2} z_{k_1} z_{k_2} \right|^q \leq \left| \frac{\lambda_f - \sqrt{\lambda_f}}{p} \max_{k_1 \neq k_2} \mathbb{E} |z_{k_1} z_{k_2}| \right|^q \leq C \left( \frac{\lambda}{p} \right)^q,$$

where we used the assumption that  $z_{k_1}, z_{k_2}$  are Sub-Gaussian and Cauchy-Schwarz inequality in the second inequality. By the Markov inequality, we get  $\left| \frac{1}{p} \sum_{k_1 \neq k_2} z_{k_1} z_{k_2} \right| \prec \frac{\lambda}{n}$  and conclude our proof.  $\square$

The following lemma is commonly referred to as the *Gershgorin circle theorem*, and its proof can be found in (Horn and Johnson, 2012, Section 6.1).

**Lemma A.3.** Let  $A = (a_{ij})$  be a real  $n \times n$  matrix. For  $1 \leq i \leq n$ , let  $R_i = \sum_{j \neq i} |a_{ij}|$  be the sum of the absolute values of the non-diagonal entries in the  $i$ -th row. Let  $D(a_{ii}, R_i) \subseteq \mathbb{R}$  be a closed disc centered at  $a_{ii}$  with radius  $R_i$ . Such a disc is called a *Gershgorin disc*. Every eigenvalue of  $A = (a_{ij})$  lies within at least one of the Gershgorin discs  $D(a_{ii}, R_i)$ , where  $R_i = \sum_{j \neq i} |a_{ij}|$ .

We then collect some important matrix inequalities. For details, we refer readers to (Ding and Wu, 2020, Lemma SI.1.9)

**Lemma A.4.** For two  $n \times n$  symmetric matrices  $\mathbf{A}$  and  $\mathbf{B}$ , we have that

$$\sum_{i=1}^n |\lambda_i(\mathbf{A}) - \lambda_i(\mathbf{B})|^2 \leq \text{tr}\{(\mathbf{A} - \mathbf{B})^2\}.$$

Moreover, let  $m_{\mathbf{A}}(z)$  and  $m_{\mathbf{B}}(z)$  be the Stieltjes's transforms of the ESDs of  $\mathbf{A}$  and  $\mathbf{B}$ , then we have that

$$|m_{\mathbf{A}}(z) - m_{\mathbf{B}}(z)| \leq \frac{\text{rank}\{(\mathbf{A} - \mathbf{B})\}}{n} \min \left\{ \frac{2}{\eta}, \frac{\|\mathbf{A} - \mathbf{B}\|}{\eta^2} \right\}.$$

## APPENDIX B. ADDITIONAL TECHNICAL PROOFS FOR SECTION 4

*Proof of Lemma 4.1.* Recall the definitions of  $\mathbf{W}_x, \mathbf{W}_y$  and  $\widetilde{\mathbf{W}}_x, \widetilde{\mathbf{W}}_y$ . Since  $p^{-1} \|\mathbf{x}_i\|_2^2 - 1 - \frac{\lambda}{p} \prec n^{-1/2}$ , it suffices to bound

$$(B.1) \quad [f'(\tau) \mathbf{O}_x - f'(2) \mathbf{O}_y] + \left[ \frac{f^{(2)}(\tau)}{2} \mathbf{H}_x - \frac{f^{(2)}(2)}{2} \mathbf{H}_y \right].$$

**Control of the first bracket of (B.1):** For the first bracket of (B.1), we have

$$(B.2) \quad f'(\tau)\mathbf{O}_x - f'(2)\mathbf{O}_y = f'(\tau)(\mathbf{O}_x - \mathbf{O}_y) + (f'(\tau) - f'(2))\mathbf{O}_y.$$

We start with providing the control of  $\mathbf{O}_x - \mathbf{O}_y$ . With the convention  $\mathbf{y}_i = (\mathbf{y}_{i1}, \dots, \mathbf{y}_{ip})$ , we find that

$$\|\mathbf{x}_i\|_2^2 - \|\mathbf{y}_i\|_2^2 = \lambda \mathbf{y}_{i1}^2.$$

Consequently, we have that  $\mathbf{O}_x(i, i) - \mathbf{O}_y(i, i) = 0$  and

$$(B.3) \quad \mathbf{O}_x(i, j) - \mathbf{O}_y(i, j) = \frac{\lambda}{p} (\mathbf{y}_{i1}^2 + \mathbf{y}_{j1}^2 - 2).$$

We can further rewrite  $\mathbf{O}_x - \mathbf{O}_y$  as

$$\mathbf{O}_x - \mathbf{O}_y = \frac{\lambda}{p} (\mathbf{1}\Phi^\top + \Phi^\top\mathbf{1} - 2\text{diag}\{\Psi\}),$$

where we recall  $\Psi = (\psi_1, \dots, \psi_n)^\top$  and  $\psi_i = \mathbf{y}_{i1}^2 - 1$  and  $\text{diag}\{\Psi\}$  is a diagonal matrix with nonzero entries  $\{\psi_i\}$ . On one hand, we have that

$$(B.4) \quad \|\mathbf{O}_x - \mathbf{O}_y\| \leq \frac{\lambda}{p} (\mathbf{1}^\top\Phi + \max_i |\phi_i|).$$

Since  $\{\psi_i\}$  are independent, by Lemma A.1, we obtain that

$$(B.5) \quad \|\mathbf{O}_x - \mathbf{O}_y\| \prec n^{-1/2}.$$

Similarly, as  $\mathbf{O}_y = \mathbf{1}\widetilde{\Phi}^\top + \widetilde{\Phi}^\top\mathbf{1}$ , where  $\widetilde{\Phi} = (\widetilde{\phi}_1, \dots, \widetilde{\phi}_n)^\top$  with  $\phi_i = \frac{1}{p}\|\mathbf{y}_i\|_2^2 - 1$ , by Lemma A.1, we find  $\|\mathbf{O}_y\| \prec \sqrt{n}$ . By (B.2), (B.5) and (4.9), we have proved that

$$(B.6) \quad \|f'(\tau)\mathbf{O}_x - f'(2)\mathbf{O}_y\| \prec n^{-1/2}.$$

**Control of the second bracket of (B.1):** For the second bracket of (B.1), we have

$$(B.7) \quad \frac{f^{(2)}(\tau)}{2}\mathbf{H}_x - \frac{f^{(2)}(2)}{2}\mathbf{H}_y = \frac{f^{(2)}(\tau)}{2}(\mathbf{H}_x - \mathbf{H}_y) + \left(\frac{f^{(2)}(\tau)}{2} - \frac{f^{(2)}(2)}{2}\right)\mathbf{H}_y.$$

We begin with  $\mathbf{H}_x - \mathbf{H}_y$  and write

$$\begin{aligned} \mathbf{H}_x(i, j) - \mathbf{H}_y(i, j) &= \mathbf{1}_{\{i \neq j\}} [\mathbf{O}_x(i, j) - \mathbf{O}_x(i, j) - 2(\mathbf{P}_x(i, j) - \mathbf{P}_y(i, j))] \\ &\quad \times [\mathbf{O}_x(i, j) - 2\mathbf{P}_x(i, j) + \mathbf{O}_y(i, j) - 2\mathbf{P}_y(i, j)]. \end{aligned}$$

When  $i \neq j$ , we have that

$$\mathbf{x}_i^\top \mathbf{x}_j - \mathbf{y}_i^\top \mathbf{y}_j = \lambda \mathbf{y}_{i1} \mathbf{y}_{j1}.$$

Consequently,  $\mathbf{P}_x(i, i) - \mathbf{P}_y(i, i) = 0$  and

$$(B.8) \quad |\mathbf{P}_x(i, j) - \mathbf{P}_y(i, j)| \prec \frac{1}{n}.$$

Similarly, by (B.3), we have

$$(B.9) \quad |\mathbf{O}_x(i, j) - \mathbf{O}_y(i, j)| \prec \frac{1}{n}.$$

Moreover, by Lemma A.1, we have that

$$|\mathbf{O}_x(i, j)| \prec n^{-1/2}, |\mathbf{P}_x(i, j)| \prec n^{-1/2}, |\mathbf{O}_y(i, j)| \prec n^{-1/2}, |\mathbf{P}_y(i, j)| \prec n^{-1/2}.$$

Together with (B.8) and (B.9), we find that

$$|\mathbf{H}_x(i, j) - \mathbf{H}_y(i, j)| \prec n^{-3/2}.$$

Hence, by Lemma A.3, we conclude that

$$(B.10) \quad \|\mathbf{H}_x - \mathbf{H}_y\| \prec n^{-1/2}.$$

Moreover, by Lemma A.1, we find that  $\mathbf{H}_x(i, j) \prec n^{-1}$ . Therefore, by Lemma A.3, we obtain that  $\mathbf{H}_y \prec 1$ . Recall (B.7). Together with (B.10) and (4.9), we find that

$$(B.11) \quad \left\| \frac{f^{(2)}(\tau)}{2} \mathbf{H}_x - \frac{f^{(2)}(2)}{2} \mathbf{H}_y \right\| \prec n^{-1/2}.$$

We can therefore conclude the proof using (B.1), (B.6) and (B.11).  $\square$

*Proof of Lemma 4.2.* The proof is similar to that of Lemma 4.1 except we need to keep close track of the role of  $\lambda$ . Especially, in light of (B.4), we have

$$\|\mathbf{O}_x - \mathbf{O}_y\| \prec \frac{\lambda}{\sqrt{n}}.$$

Consequently, we will replace (B.6) with

$$\|f'(\tau)\mathbf{O}_x - f'(2)\mathbf{O}_y\| \prec \frac{\lambda}{\sqrt{n}}.$$

Similarly, (B.8) and (B.9) should be updated as

$$|\mathbf{P}_x(i, j) - \mathbf{P}_y(i, j)| \prec \frac{\lambda}{n}, \quad |\mathbf{O}_x(i, j) - \mathbf{O}_y(i, j)| \prec \frac{\lambda}{n},$$

which leads to

$$\left\| \frac{f^{(2)}(\tau)}{2} \mathbf{H}_x - \frac{f^{(2)}(2)}{2} \mathbf{H}_y \right\| \prec \frac{\lambda}{\sqrt{n}}.$$

This concludes our proof in light of (B.1).  $\square$

DEPARTMENT OF STATISTICS, UNIVERSITY OF CALIFORNIA, DAVIS, CA, USA  
*Email address:* xcading@ucdavis.edu

DEPARTMENT OF MATHEMATICS AND DEPARTMENT OF STATISTICAL SCIENCE, DUKE UNIVERSITY,  
 DURHAM, NC, USA; MATHEMATICS DIVISION, NATIONAL CENTER FOR THEORETICAL SCIENCES, TAIPEI,  
 TAIWAN

*Email address:* hauwu@math.duke.edu